HOT WIRE ANEMOMETER TURBULENCE SURVEY OF EXPERIMENTAL COMBUSTION CHAMBER

by

John J. Morris

A Thesis Submitted to the Faculty of the

DEPARTMENT OF MECHANICAL ENGINEERING

In Partial Fulfillment of the Requirements
For the Degree of

MASTER OF SCIENCE

In the Graduate College

THE UNIVERSITY OF ARIZONA

1963

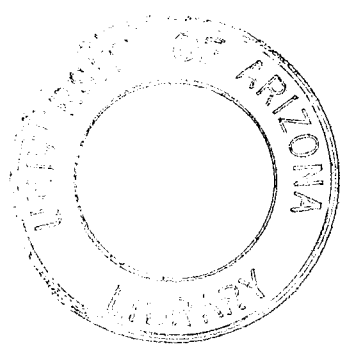
UNIVERSITY OF ARIZONA
LIBRARY

STATEMENT BY AUTHOR

This thesis has been submitted in partial fulfillment of requirements for an advanced degree at The University of Arizona and is deposited in the University Library to be made available to borrowers under rules of the Library.

Brief quotations from this thesis are allowable without special permission, provided that accurate acknowledgement of source is made. Requests for permission for extended quotation from or reproduction of this manuscript in whole or in part may be granted by the head of the major department or the Dean of the Graduate College when in their judgment the proposed use of the material is in the interest of scholarship. In all other instances, however, permission must be obtained from the author.

SIGNED John J. Morris

APPROVAL BY THESIS DIRECTOR

This thesis has been approved on the date shown below:

Russell E. Petersen
RUSSELL E. PETERSEN
Associate Professor of
Mechanical Engineering

JAN. 21, 1963
Date

ACKNOWLEDGEMENT

The author would like to express his appreciation for the guidance and assistance provided by Dr. Russell E. Petersen in the preparation of this paper.

Appreciation is also expressed to the Department of the Air Force for extending to me this opportunity for advanced study.

TABLE OF CONTENTS

NOMENCLATURE v

CHAPTER

1 INTRODUCTION 1

1.1 General 1
1.2 Description of The University of Arizona Combustion Chamber 2
1.3 Statement of the Problem 5
1.4 Selection of the Primary Instrument . 5
1.5 Principle of Hot Wire Operation . . . 6

2 EXPERIMENTAL DESIGN AND APPARATUS 12

2.1 Preliminary Considerations 12
2.2 Micromanometer 13
2.3 Hot Wire Anemometer 13
2.4 Hot Wire Probe Design and Construction 14

3 EXPERIMENTAL PROCEDURE AND SCOPE OF INVESTIGATION 21

3.1 Preliminaries 21
3.2 Obtaining the Data 22
3.3 Scope of Experimental Work 23

4 DATA EVALUATION 25

4.1 General 25
4.2 Mean Velocity Profiles 26
4.3 Turbulence Level Profiles 26

5 DISCUSSION OF RESULTS 28

5.1 General 28
5.2 Low Frequency Flow Disturbance . . . 29

TABLE OF CONTENTS
(Cont'd.)

CHAPTER

6 CONCLUSIONS AND RECOMMENDATIONS 32

6.1 Conclusions 32
6.2 Recommendations 33

FIGURES, GRAPHS, SKETCHES, PHOTOGRAPHS, TABLES . . 34

BIBLIOGRAPHY 63

NOMENCLATURE

SYMBOL	DESCRIPTION	UNITS
A	Slope of mean velocity calibration line	fps/milli-amps
A_w	Area of the hot wire	ft^2
a	Overheat ratio of an operating wire	
B	Calibration constant of RMS analyzer	
C	Constant	
c_v	Specific heat at constant volume	B/lb-F
d	Diameter	ft
E	Internal energy	ft-lb/lb
E_s	Voltage	volts
e	Unit vector	
f	Function of	
H	Magnetic field intensity	amp/meter
h	Heat-transfer coefficient	$B/sec\text{-}ft^2\text{-}F$
I	Current	amps
$\bar{I}$	Signal current of main panel meter	milliamps
$\bar{I}_c$	Calibration current of RMS panel meter	
I_t	Meter reading	
i	Heating current through hot wire	amps
j	Position indices	
l	Length	ft

m	Mass	lb
n	Integer	
Q	heat	B
R	Resistance of sensitive wire	ohms
R_o	Resistance at ambient no-flow temperature	ohms
T	Temperature of sensitive wire	F
T_o	Ambient temperature	F
U	Mean velocity past wire	ft/sec
u'	RMS of velocity fluctuation from mean	ft/sec
W	Power dissipated by hot wire	watts
α	Temperature coefficient of resistance	1/F
ϵ	Emissivity	
λ	Thermal conductivity	B/sec-ft-F
μ	Dynamic viscosity	lb-sec/ft^2
π	Constant	
ρ	Density	lb/ft^3
ρ_w	Resistivity of sensitive wire	
ρ_o	Resistivity at ambient temperature	
σ	Stefan-Boltzmann constant	B/sec-ft^2-F

CHAPTER 1

INTRODUCTION

1.1 General

The sophisticated power plants and propellants in use today have caused renewed interest in the study of the combustion process. Consequently, there has been a great expansion in the field of combustion research. One phase of this research deals with the investigation of laminar flames and the details of flame reaction. A result of this research has been the development of a very low turbulence combustion chamber. Previous to the development of this type of experimental apparatus, the measurement of flame speeds and the investigation of chemical kinetics were conducted mainly with the bomb calorimeter. (1)*

The combustion chamber provides the experimenter with a fixed steady-state flame in which many properties of the combustion process can be closely analyzed. Such studies as flame propagation, flame stability, flame front stability and the chemical kinetics of the laminar

---

* Numbers in parentheses refer to REFERENCES.

flame are being conducted at this time. Since all of these studies require a laminar flame, it is essential that a detailed examination of the fuel gas flow upstream from the actual flame be conducted.

1 2 Description of The University of Arizona Combustion Chamber

The combustion chamber designed and constructed at The University of Arizona is to be used to further the flame studies mentioned in the previous section. The design is based on a low-flow, low-turbulence test section. The most important considerations from the aerodynamic point of view are the boundary layer thickness in the test section, the flatness of the mean velocity profile, and the intensity of the turbulence present in the flow at the test section. In the general arrangement of the chamber, the following design features were incorporated to optimize the above-mentioned factors. This general arrangement is shown in Figure 1.1.

First, the boundary layer of the combustible jet was minimized by surrounding the primary combustible flow with a secondary air flow of the same velocity. This secondary flow tends to increase the stability of the primary flow. Also, the vertical design of the test section causes any buoyancy effects to be symmetric with

respect to the tunnel axis.

The reduction of turbulence has been aided by the provision of a large settling chamber upstream from the test section. This is shown in Figure 1.2. In this chamber the air is diffused, then passed through seven calming screens. The mesh size of each screen is smaller than that in the preceding screen. The screen farthest upstream is one-half inch mesh size. Its purpose is to break up any large scale eddies present into eddies of smaller size. Each succeeding screen reduces the eddy size still more until finally the mixture is passed through the fine 60 mesh per inch screen. It has been shown in experiments by Dryden (2) and Bachelor (3) that the percentage of turbulence in fluid that has been passed through such a screen series decreases to less than 1.0% at a distance equal to 200 mesh lengths from the last screen. In the combustion chamber the mixture enters a final contraction at well over this 200 mesh length distance from the final screen.

The contraction to the throat of the nozzle in Figure 1.2 is of unique design. Taken from a paper by R. Harrop (4) it is in theory analogous to the Biot-Savart theory of an electro-magnetic solenoidal field. Utilizing Biot's formula

$$H = \frac{I}{4\pi}\int_c \frac{e_r \times dS}{r^2}$$

with which it is possible to determine the magnetic field and intensity at any point due to a steady current loop, Harrop solved the equation for the case of two equal vortex rings placed axially in the earth's magnetic field. The force field was determined for a given vortex ring potential. The flux lines or lines of force were then considered as streamlines in the analogous potential flow problem and a suitable one selected as a boundary. The surface swept out by rotating this streamline about the vortex ring axis determined the boundary of the contraction cone.

Compressed air for the primary flow is supplied by a 40 horsepower positive displacement compressor located in the laboratory next to the combustion chamber. The air is delivered to a 200 cubic foot reservoir maintained at 120 psig. The air flow from this reservoir to the primary nozzle is metered at the master control panel by two Fischer-Porter Variable-area Flowmeters shown in Figure 1.3. The parallel connection of these meters, rated at 169 scfm and 36 scfm respectively, permit a coarse and fine adjustment of the flow.

The secondary air flow is provided by a large

axial-flow suction fan located on the roof of the laboratory as shown in Figure 1.1. The air is drawn from the large settling chamber at the base of the tunnel through a contraction around the primary nozzle. The placement of the fan provides positive exhaust gas expulsion as well as controlled secondary air flow. Design and construction details of the combustion chamber may be found in a Master's Thesis by N. Hicks (5).

1.3 Statement of the Problem

As mentioned previously, prior to the study of flame properties, a detailed investigation of the existing flow characteristics must be accomplished. This type of investigation requires accurate measurement of the mean velocity, turbulence (instantaneous velocity fluctuations), and certain other flow characteristics (such as effects of moisture content) that exist in and prior to the test section. It is therefore the purpose of this study to develop the instrumentation necessary to conduct such an investigation and to measure the velocity and turbulence profiles at the exit of the primary nozzle, all without flame.

1.4 Selection of the Primary Instrument

Demands upon flow instrumentation are severe; even though a device of the total-head tube or thermo-

couple type provides accurate data concerning one variable, it is incapable of providing all the required information concerning local flow characteristics. The fine wire used as a resistance thermometer or hot wire anemometer is superior to either the thermocouple or the total-head tube in fully describing the flow in the sense that it can respond much more rapidly to flow changes. The use of pressure as the primary parameter in velocity measurements places severe limitations upon the measurements of unsteady flows. A change in pressure requires some flow in or out of the pressure tube. This flow requires time and the response time to equilibrium precludes the use of pressure tubes in systems varying more than a few cycles per second (6). A wire or wire array may have very small dimensions and a response time that is measured at most in milliseconds. By proper design, the hot wire equipment is capable of yielding information about many of the important parameters influencing the flow in the combustion tunnel.

1.5 Principles of Hot Wire Operation

The hot wire anemometer is basically an indicator of the rate of heat transfer from the wire to the flowing stream. The heat loss, and hence the square of the heating current, is approximately proportional to the

square root of the gas velocity as shown by King's Equation (7).

$$\frac{i^2 R \alpha}{a} = C_1 + C_2 \sqrt{U}$$

The heat transfer from the "active" portion of the wire to the surroundings consists of conduction, convection, and radiation. An order of magnitude analysis was carried out to determine the relative importance of the various types of heat transfer. For the wire sizes used in this investigation, the result indicated that the conduction and radiation processes are insignificant when compared with convection.

The conduction process includes losses to the supports and in the case of boundary layer studies, to adjacent bodies. Since this survey is not concerned with measurements in the boundary layer, the distance to any boundary is relatively large and the error is negligible when compared with convection, and hence will not be considered.

Radiation losses are described by

$$Q = \sigma A_w \epsilon \left(T_w^4 - T_o^4\right)$$

Since the difference between the body or boundary temperatures and the wire is limited to about two hundred

degrees Centigrade and the Stephan-Boltzman constant is extremely small, the radiation losses will usually be negligible and therefore are not considered in this report.

Only the convective heat transfer is henceforth considered significant. The first law of thermodynamics states that the difference between the rate of heat transfer into the system and the rate at which work is done by the system is equal to the rate of change of internal energy in the system (6), or

$$\dot{Q} - \dot{W} = \dot{E} \tag{1-1}$$

where $\dot{Q}$ is positive for heat flow to the system and $\dot{W}$ is positive for work done by the system.

The rate of change of wire internal energy may be written

$$\frac{dE}{dt} = m\, c_v \frac{dT}{dt} = \rho \frac{\pi d^2 l}{4} c_v \frac{dT}{dt} \tag{1-2}$$

The electrical power input to the wire thermodynamically has the characteristics of work

$$\dot{W}_{in} = i^2 R \tag{1-3}$$

Substituting equations (1-2) and (1-3) into (1-1), it becomes

$$\left(i^2 R\right)_{in} = \rho \frac{\pi d^2 l}{4} c_v \frac{dT}{dt} + \dot{Q}_{out} \tag{1-4}$$

The last term $\dot{Q}_{out}$ in equation (1-4) includes the effects of both free and forced convection. At very low velocities the magnitude of the free convection term is the same order as that of the forced convection. For free convection over a horizontal cylinder, Jacob and Hawkins (8) give the following relationship

$$N_u = \frac{hd}{\lambda} = 0.525 \left(G_r \cdot P_r\right)^{0.25} \qquad (1\text{-}5)$$

The influence of the Grashof number alters the hot wire reading at very low velocities (6). The effect is shown schematically in Figure 1.4 for the condition when the forced and free convection velocity vector have an included angle of 90°. The resultant error is overcome in most hot wire equipment by calibration.

$\dot{Q}_{out}$ may now be considered forced convection only

$$\dot{Q}_{out} = h A_w \left(T_w - T_o\right) \qquad (1\text{-}6)$$

For the forced convective heat transfer process

$$N_u = f\left(Re, P_r\right)$$

and even at high velocities the Reynolds number, based on wire diameter, will remain in the laminar range. McAdams (9) determined the following empirical relationship for flow past a cylinder in the laminar range

$$\left[0.1 < Re < 1000\right], \quad \frac{Nu}{(Pr)^{0.3}} = 0.35 + 0.47\left(\frac{\rho U d}{\mu}\right)^{0.52} \qquad (1\text{-}7)$$

Since the Prantl number varies very little for gases, it can be considered as a constant (0.74) in this relationship and thus

$$N_U = \frac{h d}{\lambda} = 0.317 + 0.426\left(\frac{\rho U d}{\mu}\right)^{0.52}. \qquad (1\text{-}8)$$

Solving (1-8) for h and substituting into (1-6) gives

$$\dot{Q}_{out} = \lambda\left[0.317 + 0.426\left(\frac{\rho U d}{\mu}\right)^{0.52}\right]\frac{A_w}{d}\left(T_w - T_o\right). \qquad (1\text{-}9)$$

Equation (1-4) now becomes

$$i^2 R = \frac{\rho \pi d^2 l}{4} C_v \frac{dT}{dt} + \lambda\left[0.317 + 0.426\left(\frac{\rho U d}{\mu}\right)^{0.52}\right]\pi d l\left(T_w - T_o\right) \qquad (1\text{-}10)$$

This is the basic equation for determining hot wire characteristics.

A further relation between temperature and wire resistance is

$$R = R_o\left[1 + \alpha\left(T_w - T_o\right)\right] \qquad (1\text{-}11)$$

rearranging

$$T_w - T_o = \frac{R_w - R_o}{\alpha R_o} = \frac{a}{\alpha} \qquad (1\text{-}12)$$

where a is the overheat ratio of the constant temperature hot wire. Substituting (1-12) into (1-10) and

limiting the equation to constant temperature, it becomes

$$\frac{i^2 R \alpha}{a} = \pi l \lambda \left[0.317 + 0.426 \left(\frac{\rho d}{\mu} \right)^{0.52} U^{0.52} \right] \qquad (1\text{-}13)$$

and for any given measurement the quantities λ, ρ, and μ can be considered constants. The above equation reduces to

$$\frac{i^2 R \alpha}{a} = C_1 + C_2 U^{0.52}$$

which for practical applications can be replaced by King's Equation, in which $U^{0.52}$ is replaced by $U^{0.5}$.

CHAPTER 2

EXPERIMENTAL DESIGN AND APPARATUS

2.1 Preliminary Considerations

At the outset it was determined that the probes (hot-wire holders) supplied with the Hubbard Hot Wire Anemometer would be unsatisfactory for the type of survey to be conducted. The short length of probe, five to six inches, made it impractical to survey the closed test section. It was primarily due to this reason but also due to the circuitry of the probe that it was decided to design and construct new probes.

The proximity of the compressor and the resulting vibrations made it necessary to shut down this equipment during the actual data recording and calibration. All other equipment in the laboratory was shut down during runs to eliminate possible external noise.

It was also considered essential that the wires be calibrated in the position and flow to be studied. This was necessary since it has been found that self-induced air currents vary with probe position at very low speeds (10).

2.2 Micromanometer

The Flow Corporation Micromanometer Model MM-2 was used to calibrate and spot check the mean velocity readings of the hot wire. This is a precision instrument designed to measure small pressure differences with an accuracy of ± 0.0002 inches of manometer fluid over its entire two-inch operating range. Butyl alcohol with a density of 0.81g/cc was the manometer fluid used. See Figure 2.1.

2.3 Hot Wire Anemometer

The hot wire circuitry consisted of a Hubbard Model IIHR Type 3A Anemometer, an oscilloscope (shown in Figure 2.2 and Figure 2.3), and hot wire probes designed and built in the laboratory.

The Model IIHR Anemometer is designed for the specific purpose of measuring velocity fluctuations. Operating on the constant temperature principle, it produces a signal directly proportional to the velocity. The instrument is composed of a regulated DC power supply, twin channel control amplifiers with linearizing stages, and a root-mean-square analyzer circuit. The complete system, including probe, has a flat frequency response from 0.1 to 10 KC at the low mean velocities investigated. The upper limit is imposed by

the control system since similar types of hot wires can have frequency responses to 100 KC (11). The Hubbard Type 3A control amplifer is designed for use with a five ohm wire probe operated at an overheat ratio of .8 (approximated 210°C above ambient air temperature). Both the resistance of the wire and the overheat ratio were found to be fairly critical for obtaining a linearized response to the mean velocity due to the designed operating points of the anemometer electronic servo system.

2.5 Hot Wire Probe Design and Construction

The probes originally used in connection with the anemometer were supplied by the Hubbard Company. Typical construction of such a probe is shown in Figure 2.4. To meet the needs of this and further calibration test requirements in the combustion tunnel, a new type of probe (see Figure 2.5) was designed and built.

In the original probe, one lead from the wire mount was grounded to the probe tubing. This required selective coupling of the connectors in the probe extension cable and anemometer. Besides the inconvenience of this arrangement, common ground between the anemometer chassis and probe was sometimes difficult to maintain. The twisted piano wire mounts were found to

be unsatisfactory in both durability and rigidity.

The new probes, shown in Figure 2.5, that were constructed for use in the test section of the combustion tunnel are much longer than the original Hubbard probes. This design feature made it possible to use the ruled traversing mount on the wall of the test section as the probe holder. This, in turn, permitted complete surveys to be made in a completely closed test section (see Figure 2.6). In future investigations, ruled indices will be etched on the tubing of the probe so that it may be accurately positioned in three directions without opening the test section access doors.

Each probe was provided with a protective shield, for ease in handling, Flow Corporation Model HWS-B, shown in Figures 2.5 and 2.7. The shield consists of two sections screwed together, an outer cap (A) and an inner portion (B). The cap may be unscrewed and removed at (C). If the collet (D) is then loosened, the entire shield may be slid downward along the tube, exposing the hot wire. This shield was found to be the best means of protecting the wire from inadvertent damage. The shield may also be used to advantage both in inserting the probe into experimental equipment and positioning it for wire replacement. These uses are explained in detail in pertinent Flow Corporation Bulletins (12).

Construction details of the wire supports are shown in Figure 2.8. The supports used were nickel-plated steel sewing needles 0.028 inches in diameter below the tapered ends. These needles were then forced through 0.027 inch diameter holes symmetrically drilled in a lucite plug. The drilled holes were spaced a distance of 0.125 inches center to center. After soldering the lead wires to the supports, the lucite plug, which was tapered for a force fit into the end of the tubing, was coated with Epoxy Resin and inserted.

The entire wire mounting and etching procedure is described in some detail because the satisfactory instrument operation is critically dependent upon probe construction.

For ease in working, the probe was securely fastened in the vertical position. A hole drilled in the work table fitted with a plate tapped to accommodate the threaded shield proved convenient for positioning.

The mounts were then treated with an acid flux and tinned. When tinning the mount was stroked from the base to tip with the iron so that a small amount of solder was deposited on the tip of the mount. The wire was handled fairly easily with a pair of small tweezers. A right angle bend was made near the free end of the

wire, then the wire positioned as in Figure 2.8b. The soldering iron was then brought to position 1, pinching the wire between the iron and mount. To imbed the wire in the solder at the tip of the mount, it was necessary to hesitate only momentarily at this position, then to stroke smoothly downward to attach the wire for a portion of the mount length. The wire is then positioned across the tip of the opposite mount and down its length. Maintaining a slight amount of tension on the wire and applying the soldering iron to position 2, as was done with the first mount, results in maximum contact area and support.

Wollaston wire, silver plated platinum was used exclusively in this experiment. The overall diameter is 0.001 inches with a 0.00014 inch diameter platinum core.

The design operating wire resistance for use with the Type 3A Control Amplifier is five ohms. Completely etching the silver from the wire core, to produce this resistance, would expose an "active" wire length of 0.001 inches. This order of length is both difficult to obtain and impractical for use in the type of survey conducted. Therefore, a practical "active" length was determined, which is discussed next.

Even though the anemometer is called a constant

temperature or constant resistance type instrument, velocity fluctuations can generate a signal only by changing the temperature, and hence the resistance, of the sensing element (13). The equilibrium or steady-state relationship between temperature and velocity is a function of fluid properties and operating temperatures but is not dependent upon the material properties of the sensing element. The change in signal voltage ΔE_s which results from a given temperature change is

$$\Delta E_s = i \Delta R = i R \alpha \Delta T$$

where i is constant during a short time in which the sensing elements interpret the change.

Since $$R = \frac{4 l \rho}{\pi d^2}$$

E_s becomes

$$\Delta E_s = i \left(\frac{4 l \rho}{\pi d^2} \right) \alpha \Delta T \qquad (2\text{-}1)$$

The power dissipation is also independent of the wire properties and

$$\dot{W} = i^2 R$$

Therefore

$$i = \sqrt{\frac{\dot{W}}{R}} = \sqrt{\frac{\pi d^2 \dot{W}}{4 \rho l}} \qquad (2\text{-}2)$$

Combining equations (2-1) and (2-2) yields

$$\Delta E_s = \left[\frac{4\dot{W}l\rho}{\pi d^2}\right]^{1/2} \alpha \Delta T \qquad (2\text{-}3)$$

Now utilize the relationship for the overheat ratio that

$$a = \frac{R - R_o}{R_o}$$

in which R_o is wire resistance at ambient no-flow temperature. This also can be written

$$a = \frac{\rho_w - \rho_o}{\rho_o} \qquad (2\text{-}4)$$

and substituting leads to a final relationship that

$$\Delta E_s = \left[\frac{4\dot{W}l}{\pi d^2}\right]^{1/2} \left[\rho_o \alpha^2 (1+a)\right]^{1/2} \Delta T \qquad (2\text{-}5)$$

It is apparent from the above equation that the terms $(\rho_o \alpha^2)^{1/2}$, $(1/d^2)^{1/2}$, and a can be considered as the basic criteria of sensitivity. A compromise between the requirements for sensitivity and spacial resolution resulted in the selection of 0.1 inch for the "active" wire length. It was subsequently discovered that shortening the active length adversely affected the linearity of response in the low velocity range.

Prior to etching, the mounts were completely coated with paraffin to protect them from the nitric acid used in etching.

For the etching process, the anemometer bridge was used with a bridge current of 0.5 ma and the galvanometer was replaced by a more sensitive microammeter (25 ua full-scale). Then the appropriate resistance was set in the variable leg of the bridge and the wire immersed in a three-quarter strength solution of nitric acid. At the first indication of galvanometer current change, the action was stopped by immersing the probe in water, and the acid solution was changed to half-strength. The half-strength solution slowed the process and reduced the chances of overshooting the desired resistance.

When the etching process was completed and the wire had been washed in water, the paraffin was removed from the mounts. A small soldering iron and variac proved most effective for this operation. By maintaining the temperature of the iron well below that of the solder melting point, the paraffin was easily melted from the mounts.

CHAPTER 3

EXPERIMENTAL PROCEDURE AND SCOPE OF THE INVESTIGATION

3.1 Preliminaries

Accurate determination and evaluation of flow data required that all possible sources of error be either eliminated or rigidly controlled. Inaccurate positioning of the probe, variation of the mean flow in the nozzle, and external noise were found to affect the readings.

As described in the previous chapter, the probe was held in the flame-holder mount. The axis of the wire was then carefully positioned with the aid of a magnifying glass to insure that the wire was normal to the nozzle flow.

The sensing wire was found to respond to external noise in the laboratory. The greatest source of this noise was the air compressor. Therefore, the reservoir was pressurized to capacity and the compressor shut down prior to any wire calibration or turbulence survey. It was then found that this procedure induced another source of error. As the pressure in the reservoir decreased, the pressure regulator failed to maintain constant low pressure at the nozzle. This necessitated

constant checking of the flow and adjustment of the flowmeters before each reading.

Magnesium oxide particles used in conjunction with particle track measurements were found to have been deposited in the settling chamber and clogging the fine-mesh screens. It was essential to completely remove this oxide from the system, for in addition to defeating the purpose of the screens, the particles carried along with the stream could cause impact errors (10) in turbulence measurements, and steady flow measurement errors by coating the wire (9).

3.2 Obtaining the Data

The wires were calibrated at the mouth of the combustion tunnel primary nozzle while held in the same mount that was used for the later turbulence survey. This procedure will be of greater importance in future investigations at low air speeds since at these low air speeds self-induced air current varies with the probe position (10). The micromanometer pitot tube and the probe were symmetrically positioned with respect to the nozzle. Care was exercised to assure that the pitot tube and probe were separated by sufficient distance to prevent either one from disturbing the flow past the other. The anemometer current meter was then

adjusted for full-scale reading at 30 fps flow as measured by the micromanometer. Simultaneous readings of the meter current $\bar{I}$ and the velocity U were then taken as the velocity was reduced in increments at the panel board. A secondary check was made with the readings of the control panel flow rate meter and good agreement was found. A plot of U versus $\bar{I}$, micromanometer readings versus anemometer current readings for several different wires, is shown in Figure 3.1.

After completion of a wire calibration, the probe was positioned at the center of the nozzle, a predetermined height above the lip. The flow was then adjusted and maintained constant at the panel board while the probe was traversed. The initial reading of $\bar{I}$ and I_t were taken at this center position, which corresponds to position 1 in Tables 3.1. The traverse was accomplished on one-eighth inch increments from position 1 to position 14, then in one-sixteenth inch increments to position 18. Traverses were made at levels of one-sixteenth, one-eighth, one, and two inches above the mouth of the nozzle.

3.3 Scope of Experimental Work

Including preliminary calibrations and traverses that were made before satisfactory U versus $\bar{I}$ curves

were obtained, eight calibrations and ten traverses were made. After cleaning the screens and obtaining linear wire response, velocity and turbulence measurements were concentrated near the exit of the nozzle with sample runs being made at the one and two inch level.

CHAPTER 4

DATA EVALUATION

4.1 General

An examination of the curves plotted in Figures 3.1 and 4.1 shows that although the wire response to air velocity appears to be approximately linear over a large portion of the flow range for each wire calibrated, there is a slight change in slope. For extreme accuracy it is apparent that a point or tangential slope for each reading should be determined. For this survey, use of the average slope in the middle or linear portion for each wire calibrated was considered adequate for the majority of readings. The micromanometer is accurate to within 2.5%. Since the wire response was calibrated against this instrument and the anemometer has a flat frequency response from 0.1 to 10 KC, an overall system accuracy of 5% is estimated.

Air properties, including humidity, varied only slightly during the survey. The humidity was consistently below thirty percent and was considered to have no effect on turbulence measurements or the steady flow measurements at the low velocities investigated (10).

4.2 Mean Velocity Profiles

A profile of the mean velocity was plotted in conjunction with each turbulence profile. These plots are shown in Figures 4.2 through 4.5.

Having determined the slope

$$A = \frac{\Delta U}{\Delta \bar{I}}$$

for the wire in use (Figure 3.1), the product of the meter current $\bar{I}$ and the slope value was used to determine the local mean velocity at each position

$$U_j = A \bar{I}_j$$

The plot of local mean velocities shows a flat velocity profile close to the nozzle outlet. This profile confirms the work done by Hicks (5).

4.3 Turbulence Level Profiles

The turbulence level indications were obtained by use of the RMS Analyzer incorporated in the anemometer circuitry. The wire signal is fed to the analyzer, then amplified and integrated such that the panel meter reading I_t has the relationship

$$BF\, I_t = \left[\overline{(I - \bar{I})^{1/2}} \right]^{1/2}$$

B is a calibration constant for the meter defined as

$$B = \frac{0.01}{I_c}$$

and is determined by activating a fixed internal signal in the analyzer, then adjusting the circuit gain for a desired B . For this survey, I_c was adjusted to give a full-scale reading of 5 ma for a B value of 0.002. (13).

The values of F are fixed at 1, 2, 4, 8, 16 and 32 and are controlled by the multiplier selector on the analyzer panel.

At each position, then, $\overline{I}$ and I_t are obtained from the anemometer meters and are related to U and u' by

$$U = A\,\overline{I}$$

$$u' = A\left[\overline{(I-\overline{I})^2}\right]^{1/2}$$

or

$$u' = ABF\,I_t$$

Plots of the resulting data are shown in Figures 4.6 through 4.10.

CHAPTER 5

DISCUSSION OF RESULTS

5.1 General

Although the linear characteristics of the probes used in this survey were fairly consistent, a closer examination of probe number four shows a slight increasing gradient above 20 fps air velocity and a zero velocity reading of 1.2 ma. This departure from linear response was much more apparent in several wires. In each case, a microscopic examination of the active portion showed uneven etching where a very short section of the wire appeared to be etched down to the platinum core and other sections etched little, if at all. This extremely uneven surface tended to produce marked temperature gradients in the active portion of the wire, and could increase the loss by conduction to the mounts and alter the designed convective heat transfer relationship between the wire and the anemometer.

Several unsuccessful attempts at etching were due to the wire failing in tension before any reduction in wire area could be detected in the bridge balance. These failures are believed to be caused by faults in

the wire, most likely to discontinuity in the platinum core. Such failures are unavoidable but indicate the wire spool should be handled with great care and unnecessary bending of the wire avoided.

5.2 Low Frequency Flow Disturbance

A comparison of the turbulence curves presented here with those obtained from the nozzle of a similarly designed combustion tunnel (12) indicate the level of the flow disturbance found in The University of Arizona tunnel to be extremely large. It is obvious from the oscilloscope photographs shown in Figure 5.1 that although the profiles presented indicate the actual level of the disturbance found, this disturbance is not entirely due to random velocity fluctuations or "true" turbulence. The photos show that the characteristic turbulence fluctuations are superimposed on a large amplitude, low frequency disturbance. Investigation showed that the frequency of this disturbance, approximately 33 cps, was independent of the nozzle air velocity but that the amplitude of the signal varied directly as the air velocity. This exact signal was observed with every probe introduced in the primary flow, but was absent in the secondary flow. This investigation was the first of the preliminary steps taken to

isolate the source of the disturbance.

A filter was incorporated into the anemometer circuitry between the output of the main amplifier and the RMS Analyzer input to block this low frequency. Several trial readings were then attempted at the 1/16 inch level. The oscilloscope showed the same amplitude of "true" turbulence as observed in previous readings but this disturbance was below the sensitivity of the RMS Analyzer and could not be detected on the panel meter. Since the minimum readable I_t is 0.1 and the flow was set at 20 fps, this indicates the percent of true turbulence present in the flow to be .03 or less. This value is of the same magnitude as that found in other similarly designed tunnels.

Since this 33-cycle noise introduces an order of magnitude increase in the observed disturbance in the range of flows that will be used for flame studies, it is deemed essential that this noise either be eliminated or substantially suppressed.

The most probable cause of the disturbance is acoustical noise. Two possible sources were checked. First an "organ pipe" effect of the exhaust duct was checked. Opening both the lower test section access doors and the upper vent slides, which radically changed the duct's effective length, had no effect on

the signal.

The next source considered was the possible vibration of the pressure regulator diaphragm. To check this, the entire control panel was by-passed and the air piped from the reservoir directly to the settling chamber. This modification also had no effect on the disturbance.

The preliminary two checks apparently have determined the source location to be between the inlet pipe to the settling chamber and the nozzle exit. The precise determination and elimination are left for a later study.

CHAPTER 6

CONCLUSIONS AND RECOMMENDATIONS

6.1 Conclusions

There is present in the primary flow a low frequency disturbance. The fixed frequency and varying amplitude of the disturbance at different flow rates indicate that the disturbance is acoustic noise. It apparently originates either in the settling chamber or settling chamber lead-in pipe.

The mean-velocity surveys indicate a sufficiently flat velocity profile in the test area for flame speed studies. The results of the turbulence survey plus the investigation of the low frequency disturbance indicated by the scope photography show a very low level of actual turbulence present in the primary flow.

If the 33-cycle noise signal originates below the contraction (as is quite likely) we have in effect a resonance chamber with the contraction acting as a sound receiver. Qualitatively, it seems that the contraction acts as a horn, collecting and concentrating the sound.

6.2 Recommendations

First priority must be given to eliminating the acoustic noise. The presence of this disturbance introduces a pulsation that will effect the stability of the laminar flame. A thorough investigation of the noise with available acoustic measuring instruments is recommended.

After the installation of calming screens in the entrance of the secondary contraction, an investigation of the reduction of shear effects by flow matching of the primary and secondary air should be undertaken.

Finally, in conjunction with the above study and other investigations, improved methods and techniques for wire mounting should be developed. Construction of a jig for aiding wire attachment and improving the method of mount protection during the etching process should be considered.

6.2 Recommendations

First priority must be given to eliminating the acoustic noise. The presence of this disturbance introduces a pulsation that will effect the stability of the laminar flame. A thorough investigation of the noise with available acoustic measuring instruments is recommended.

After the installation of calming screens in the entrance of the secondary contraction, an investigation of the reduction of shear effects by flow matching of the primary and secondary air should be undertaken.

Finally, in conjunction with the above study and other investigations, improved methods and techniques for wire mounting should be developed. Construction of a jig for aiding wire attachment and improving the method of mount protection during the etching process should be considered.

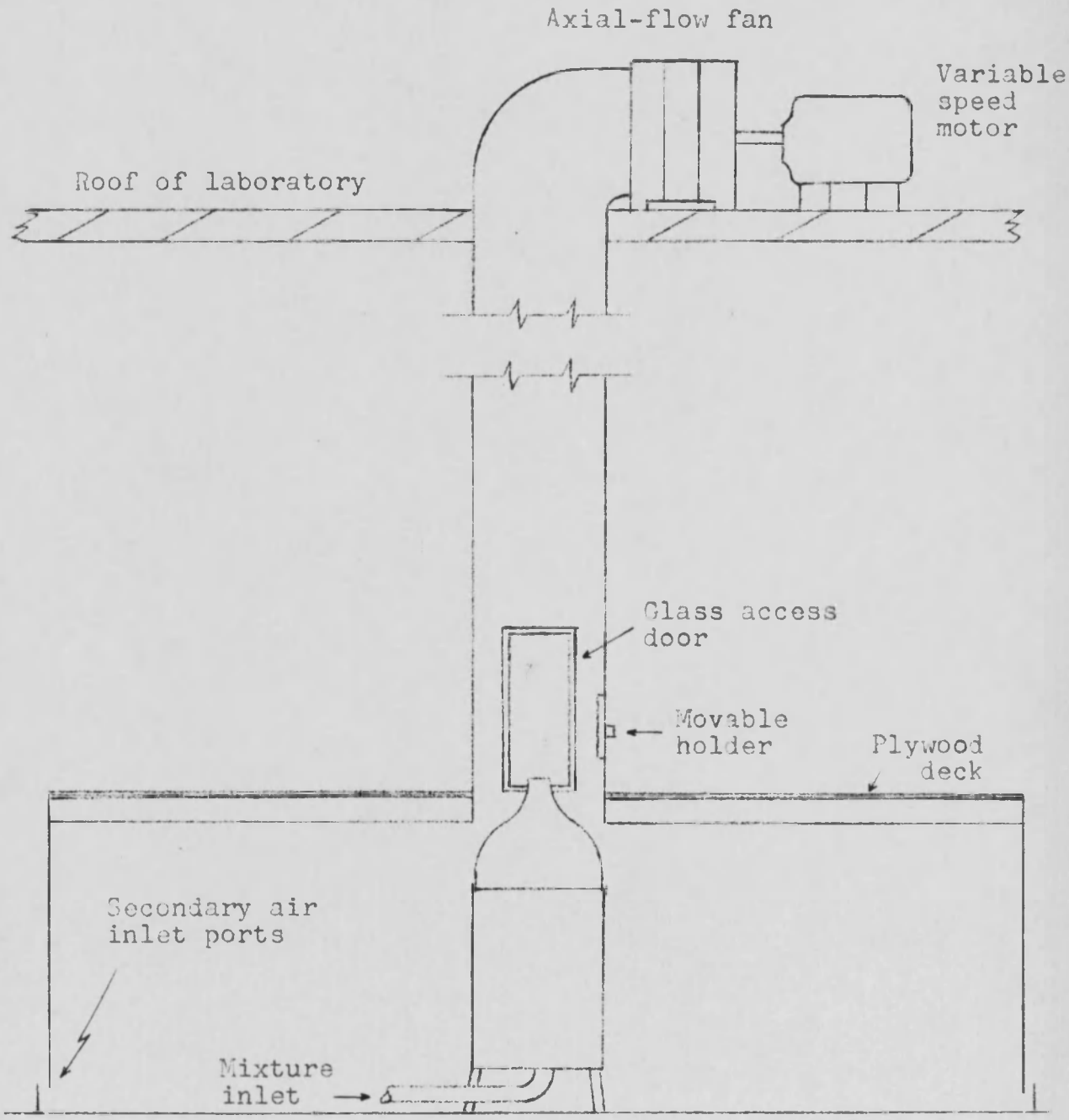

FIGURE 1.1

COMBUSTION CHAMBER GENERAL ARRANGEMENT

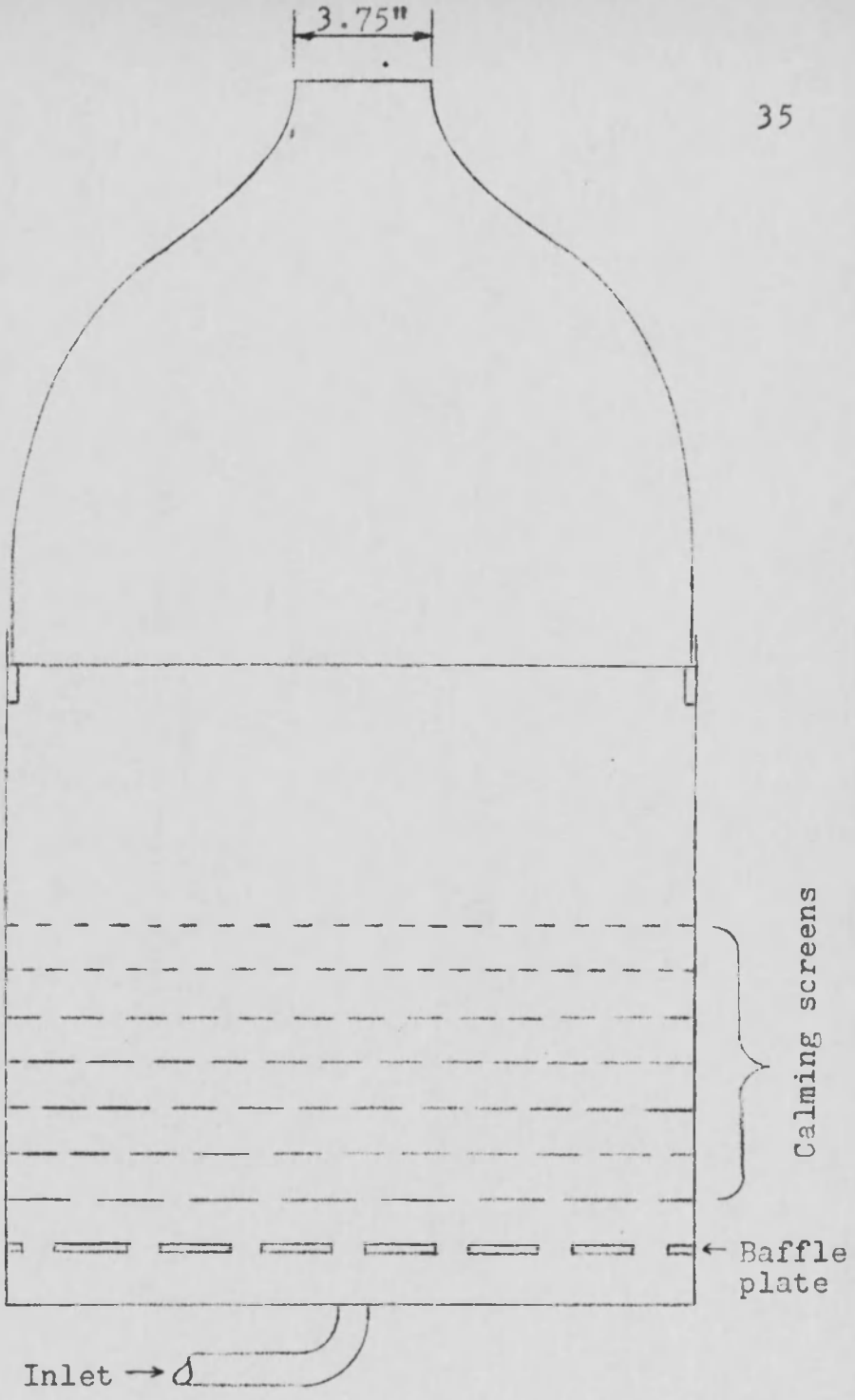

FIGURE 1.2

SETTLING CHAMBER AND NOZZLE

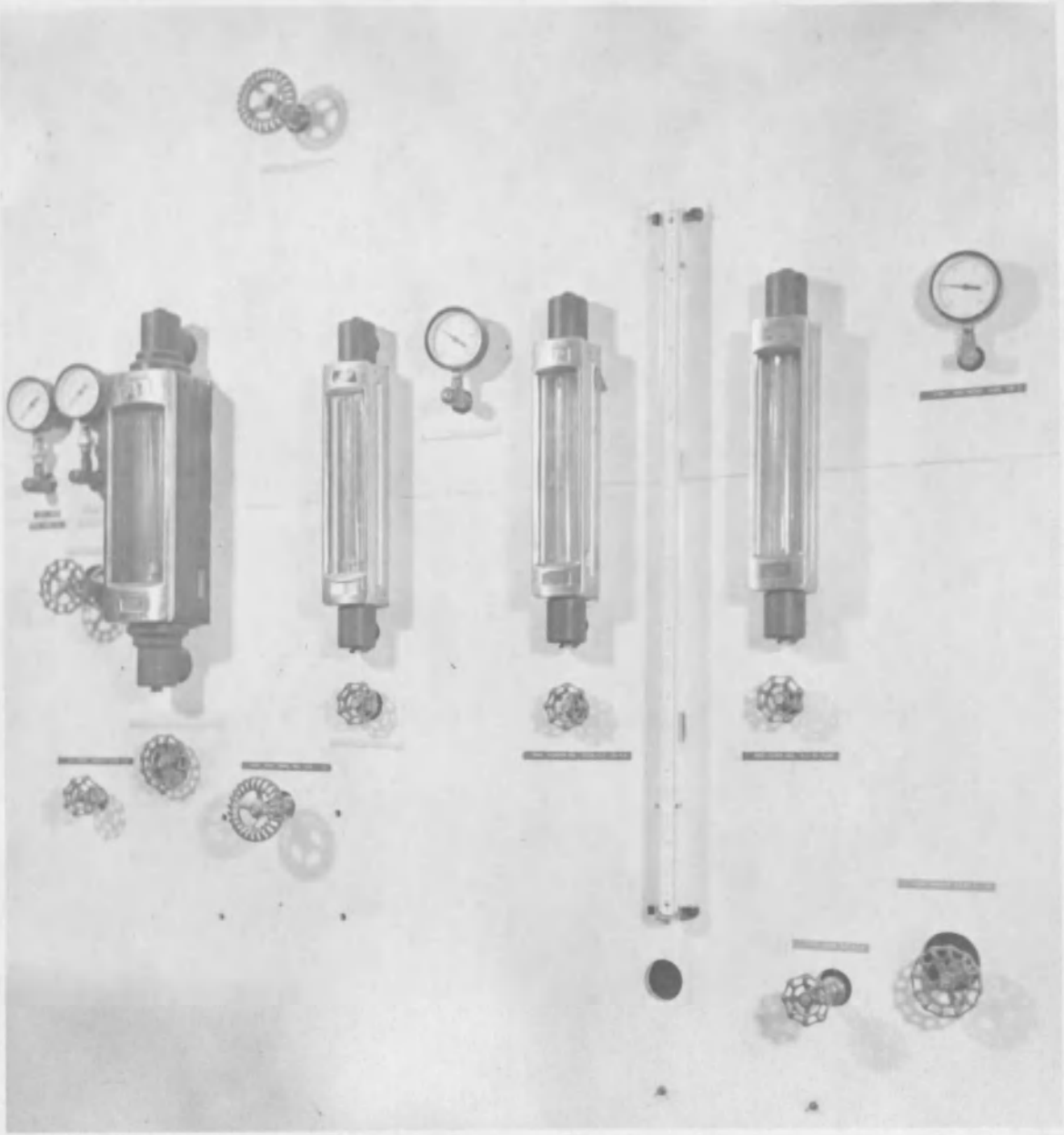

FIGURE 1.3

MASTER CONTROL PANEL

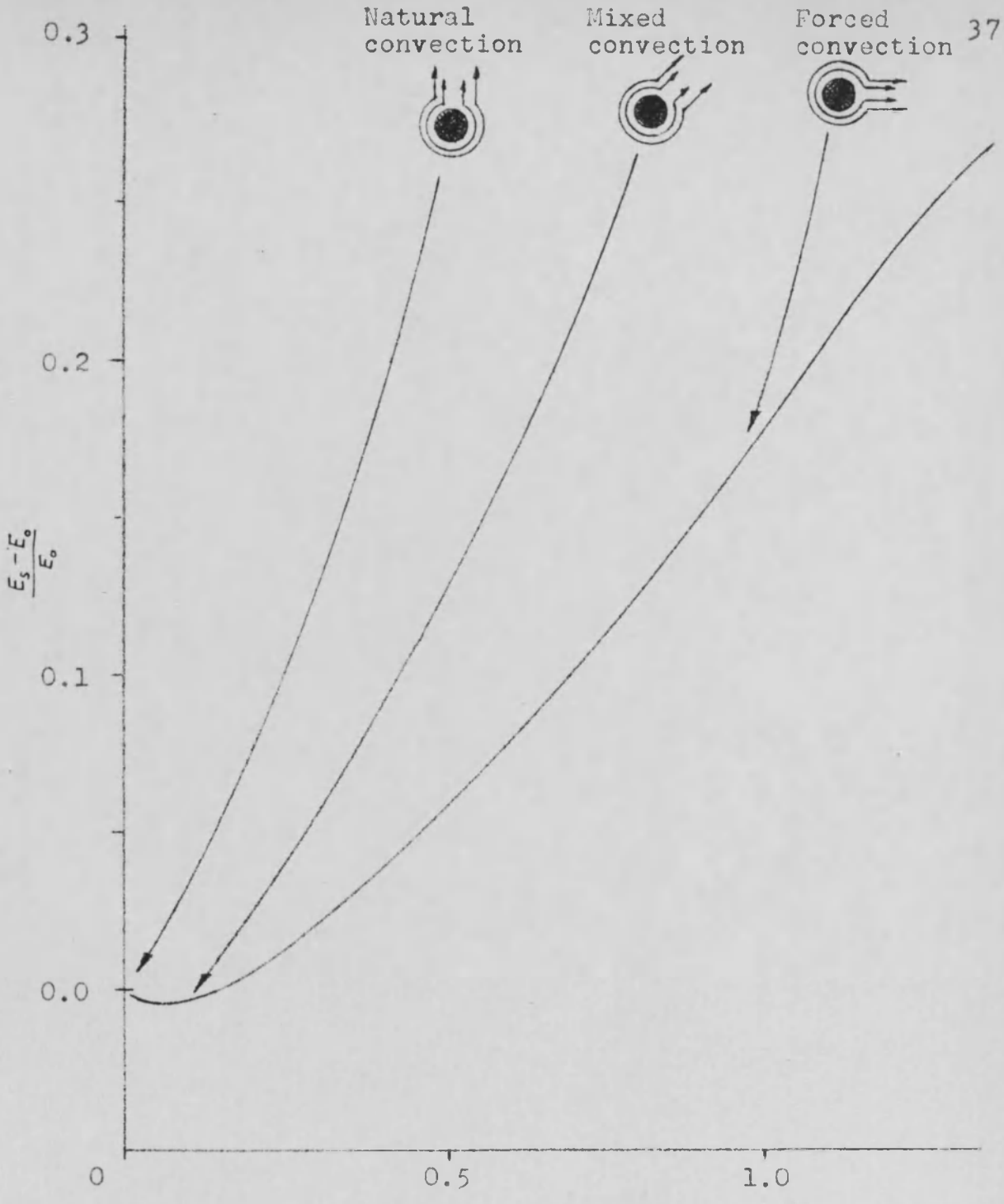

FIGURE 1.4

HOT WIRE CHARACTERISTICS AT VERY LOW VELOCITIES

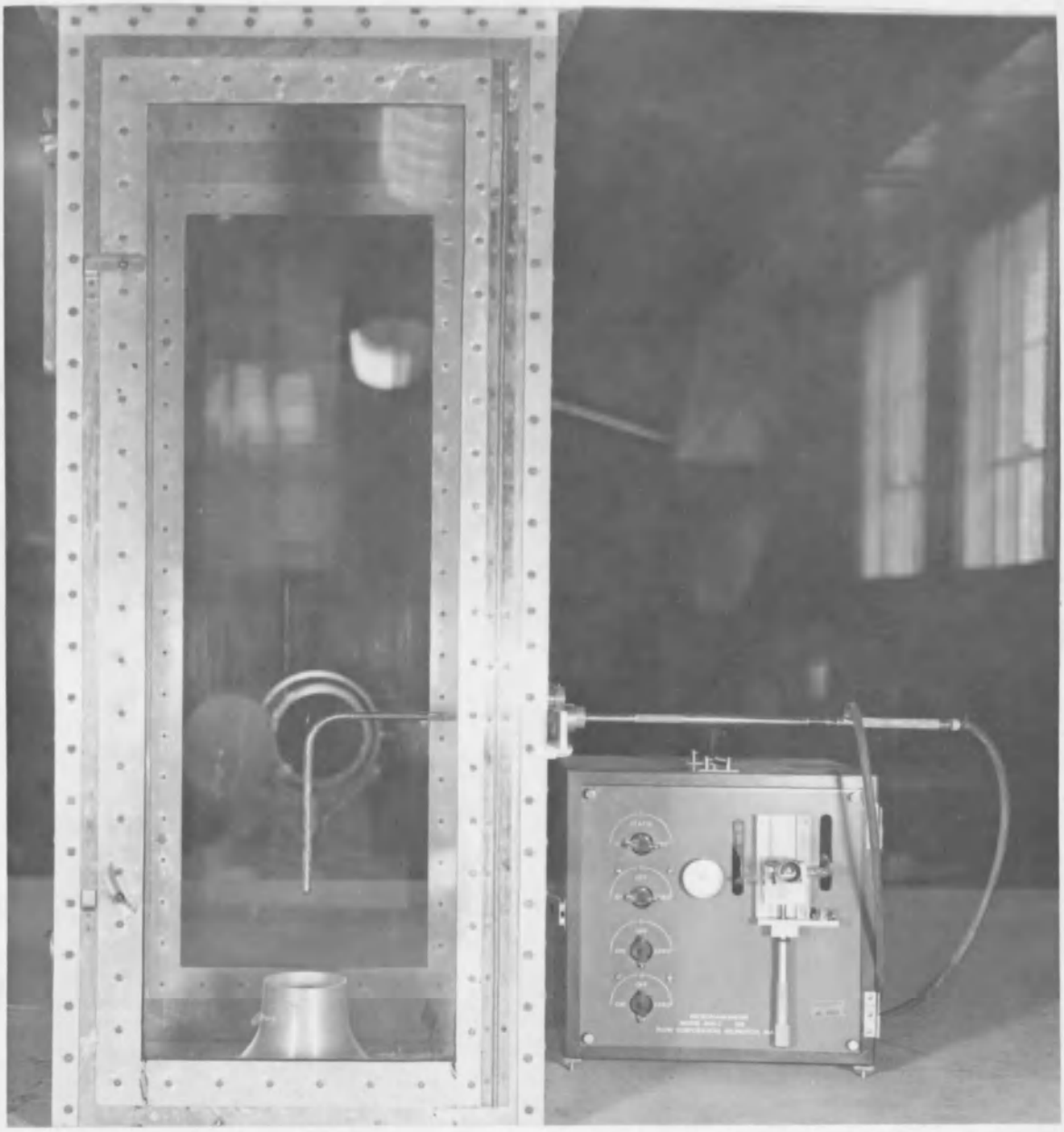

FIGURE 2.1

MICROMANOMETER AND PITOT TUBE

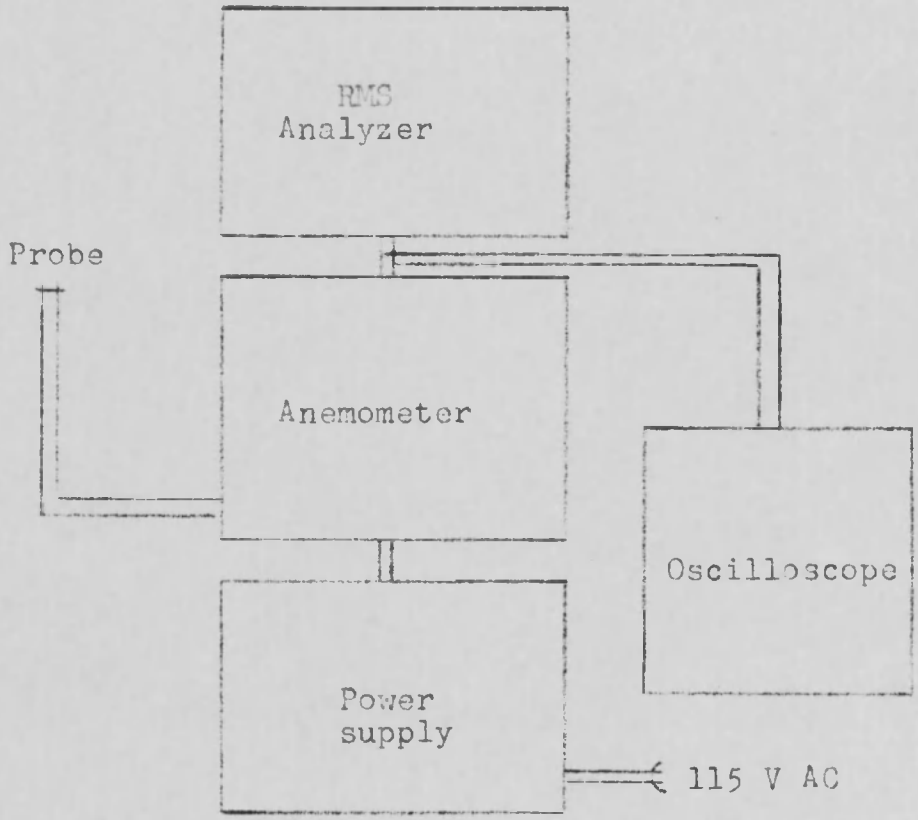

FIGURE 2.2

BLOCK DIAGRAM OF HOT WIRE CIRCUITRY

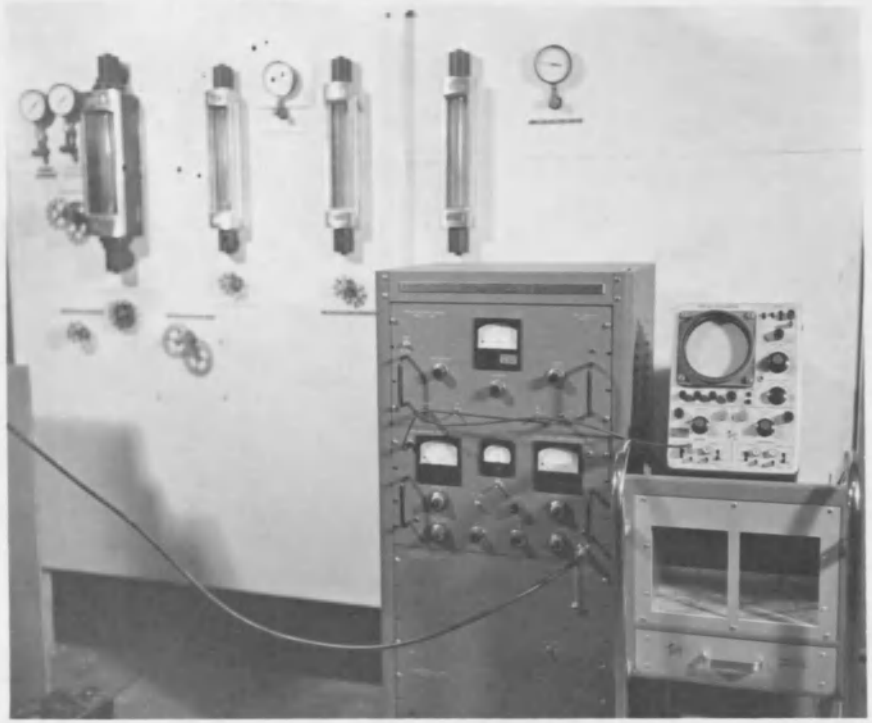

(a)

Test position

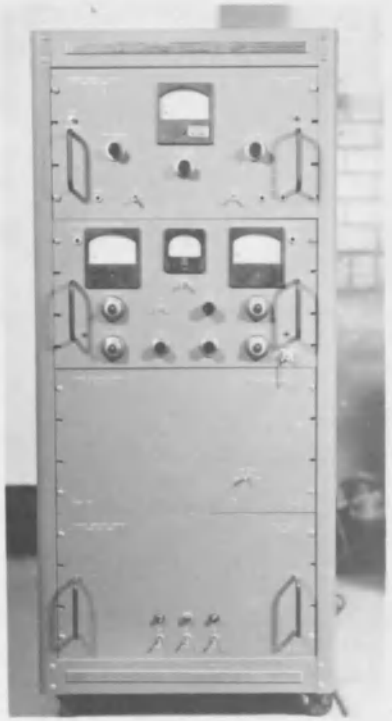

(b)

Anemometer
control panel

FIGURE 2.3

ANEMOMETER, RMS ANALYZER AND OSCILLOSCOPE

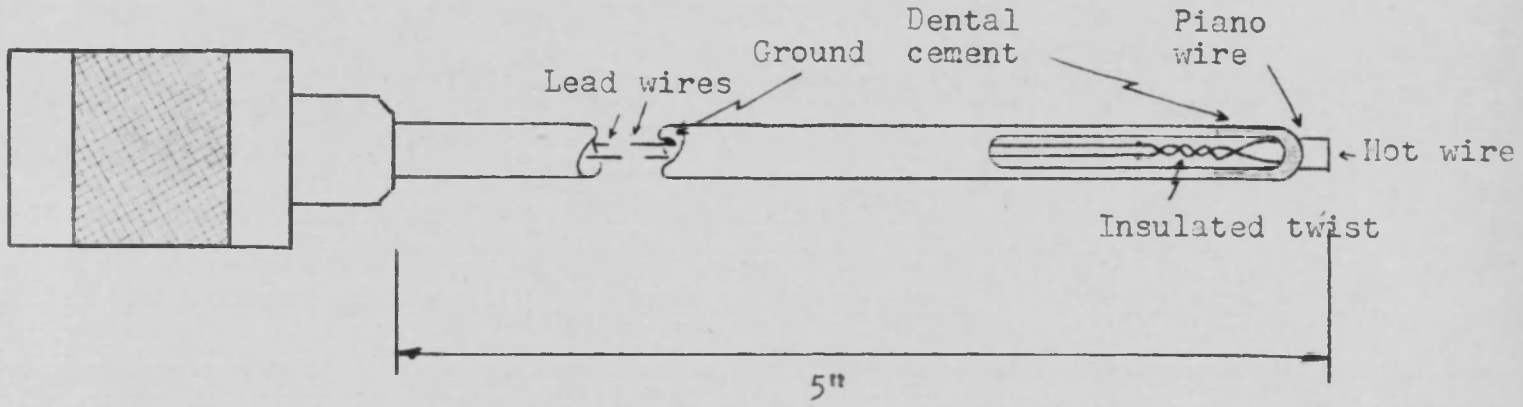

FIGURE 2.4

HUBBARD PROBE CONSTRUCTION DETAILS

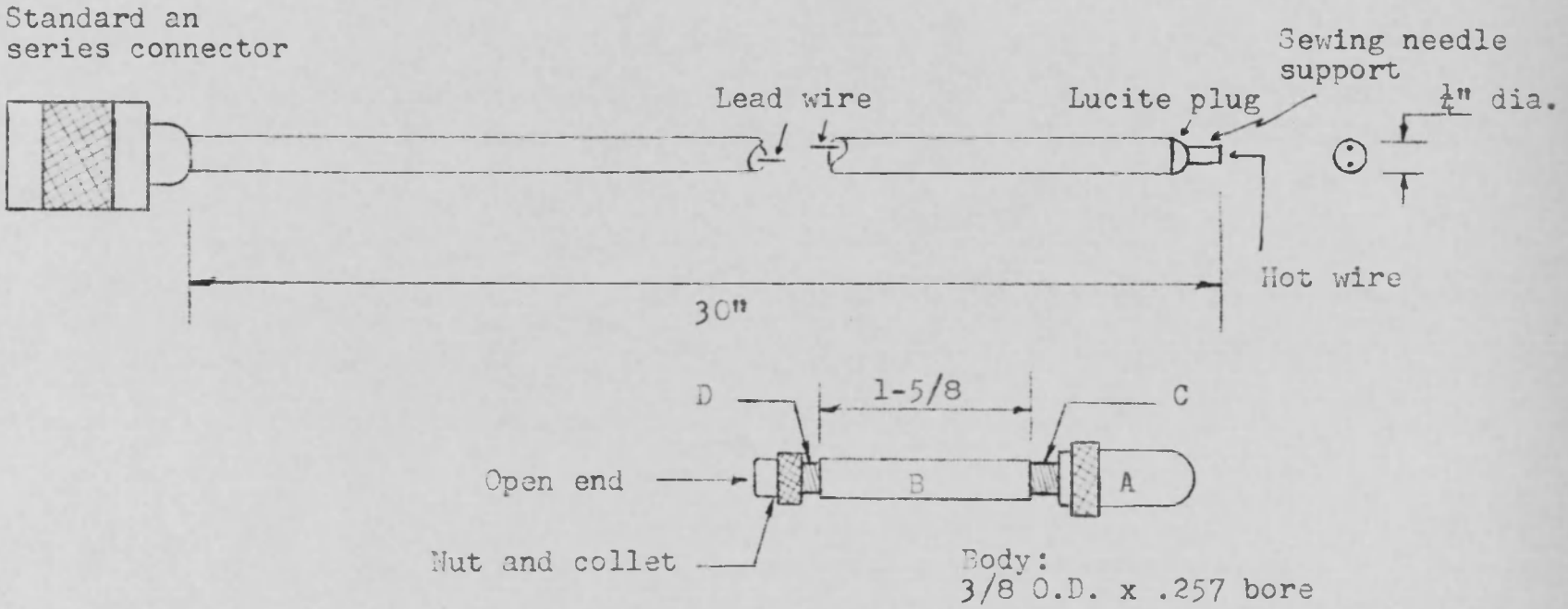

FIGURE 2.5

CONSTRUCTION DETAILS OF COMBUSTION TUNNEL PROBE AND SHIELD

FIGURE 2.6

COMBUSTION PROBE IN TEST POSITION

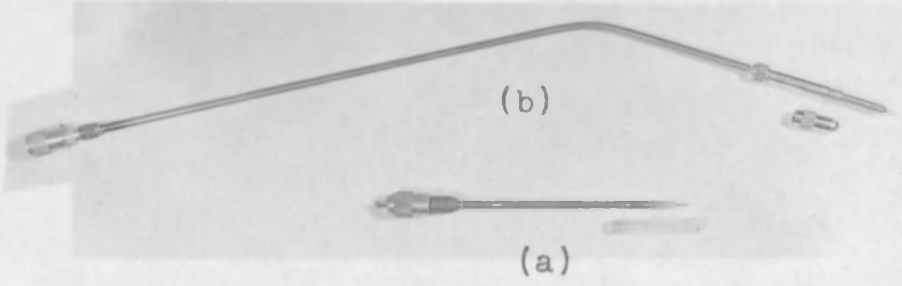

FIGURE 2.7

HUBBARD (a) AND COMBUSTION PROBE (b)

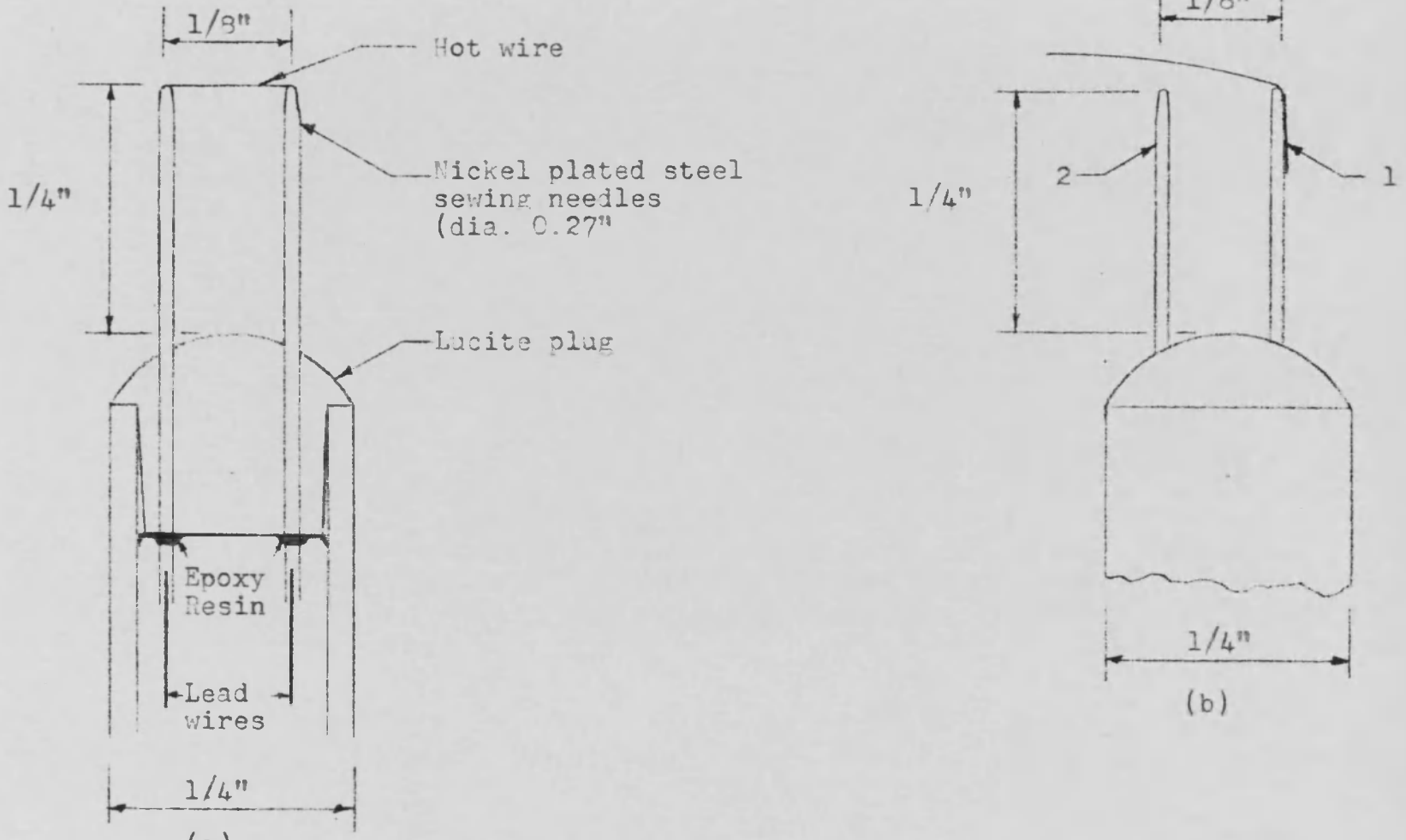

FIGURE 2.8

PROBE CONSTRUCTION DETAILS

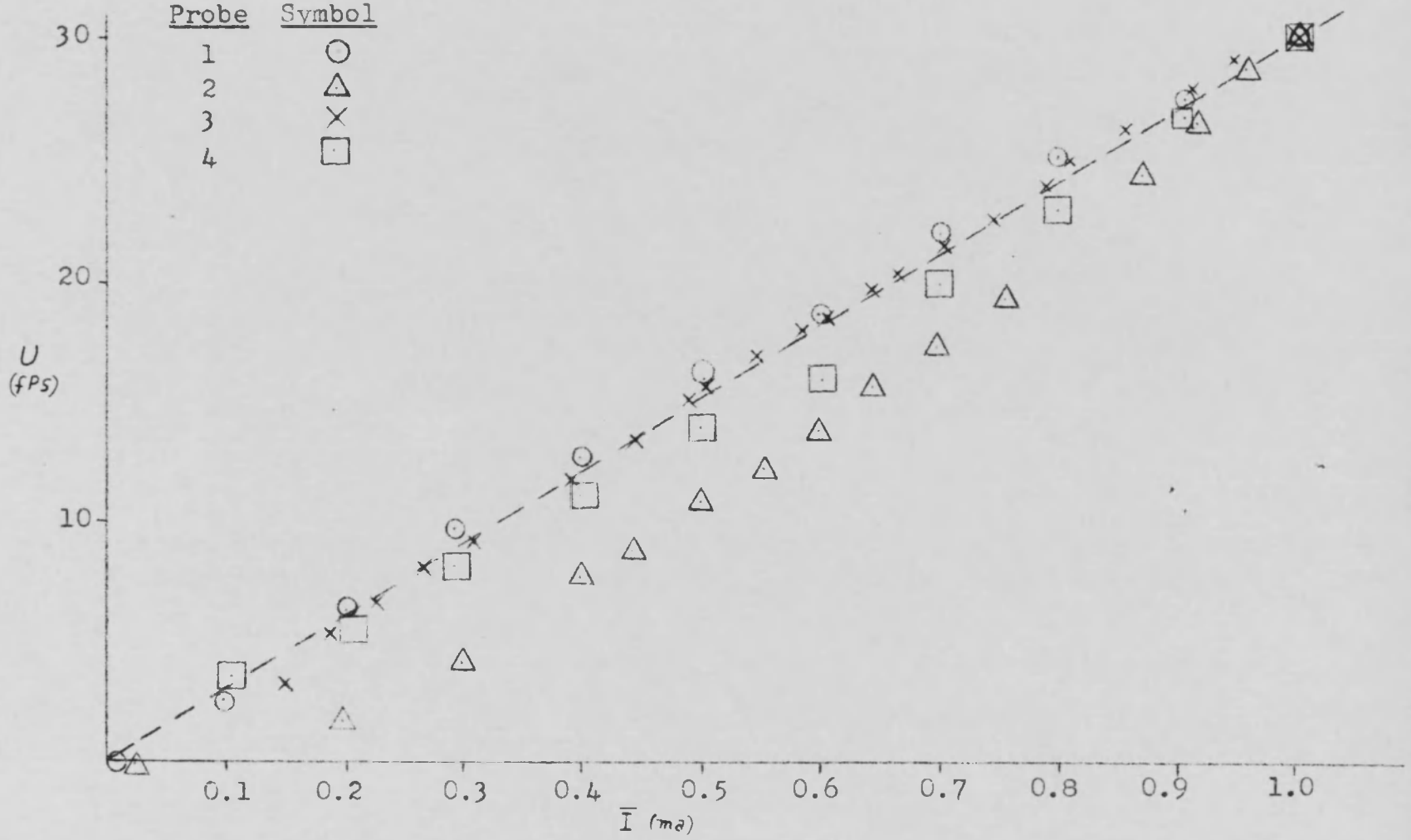

FIGURE 3.1

HOT WIRE CALIBRATION CURVES

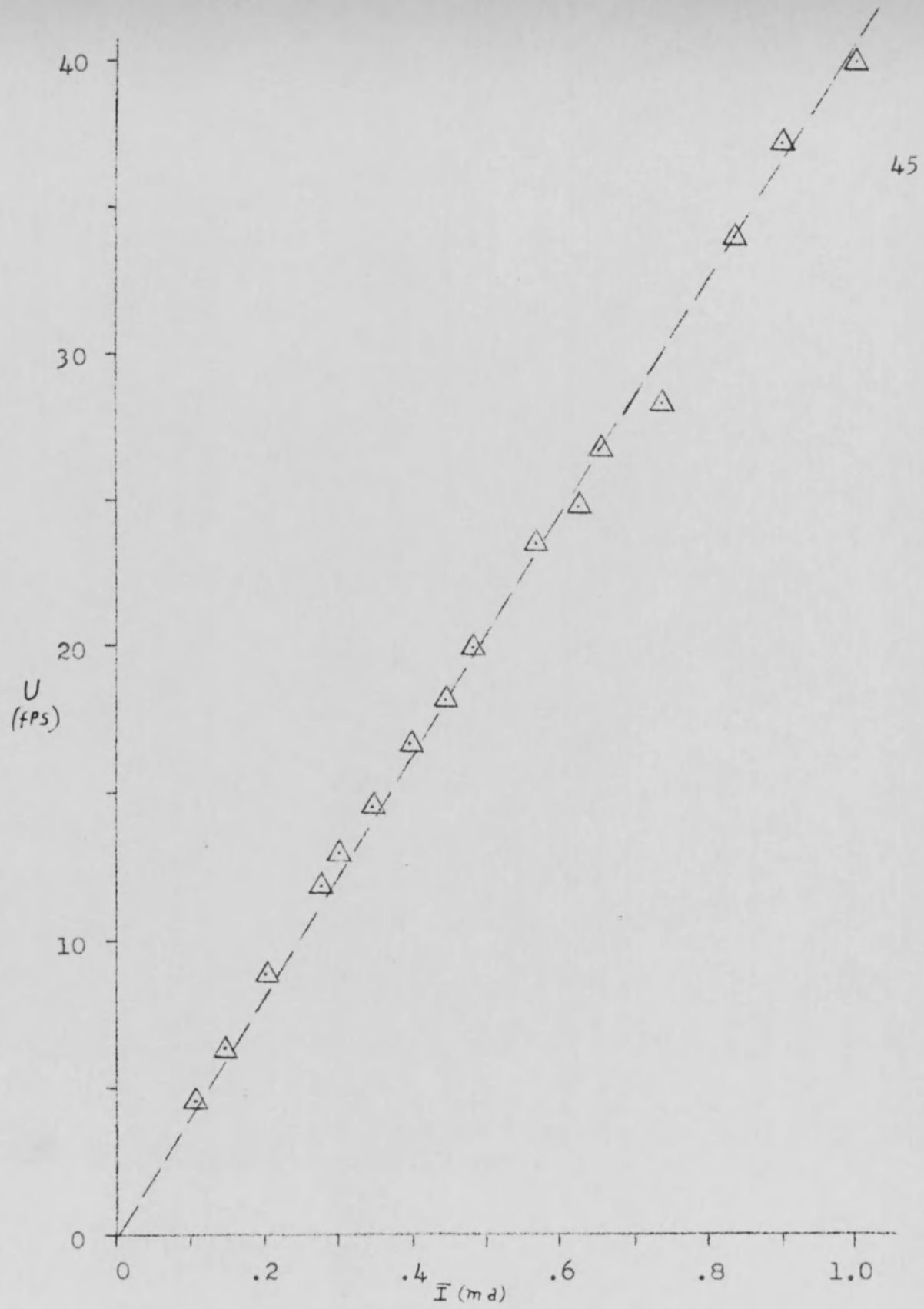

FIGURE 4.1

VELOCITY VS CURRENT CURVE FROM 0-40 fps

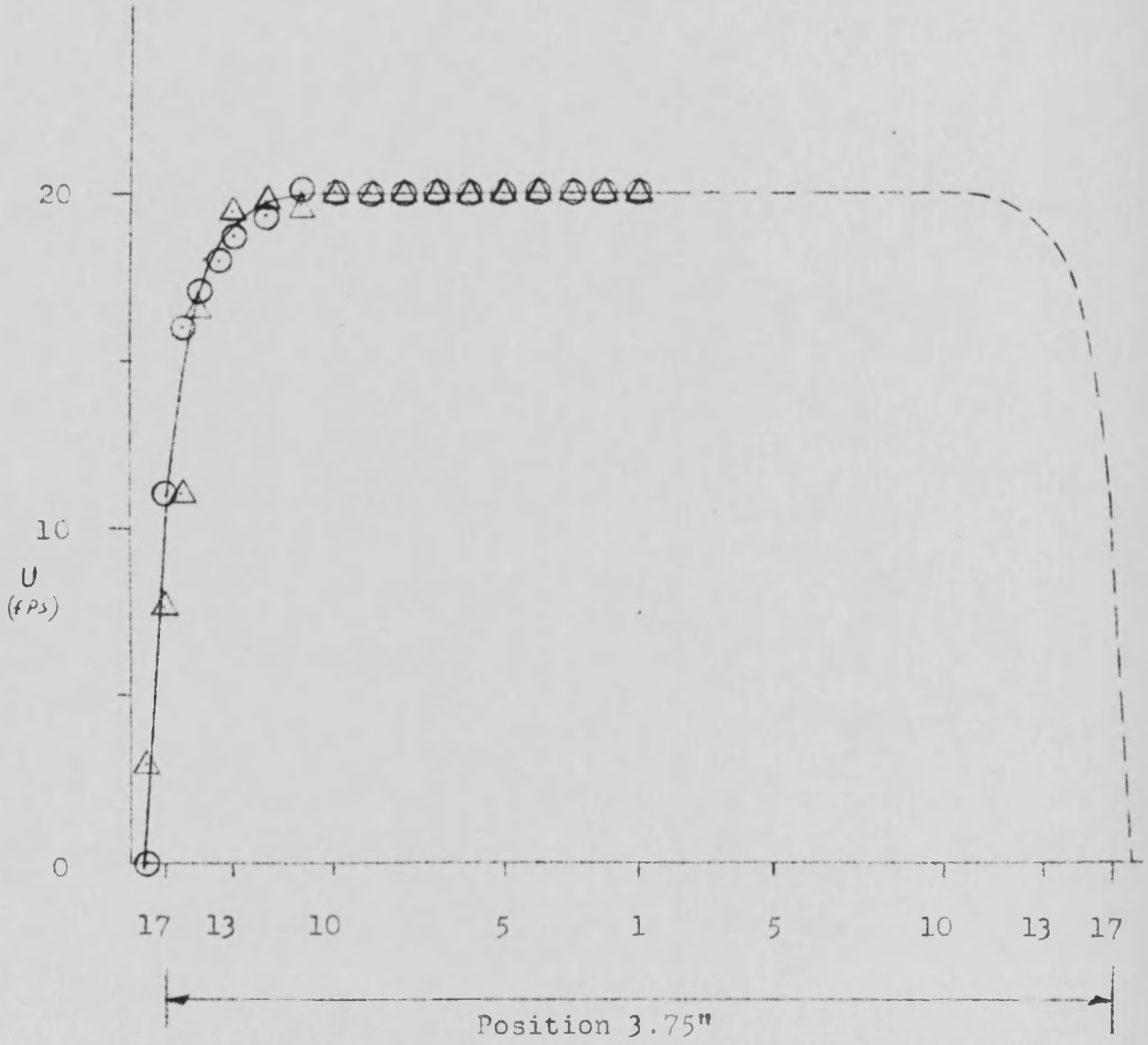

FIGURE 4.2

MEAN VELOCITY PROFILE 1/16" ABOVE NOZZLE

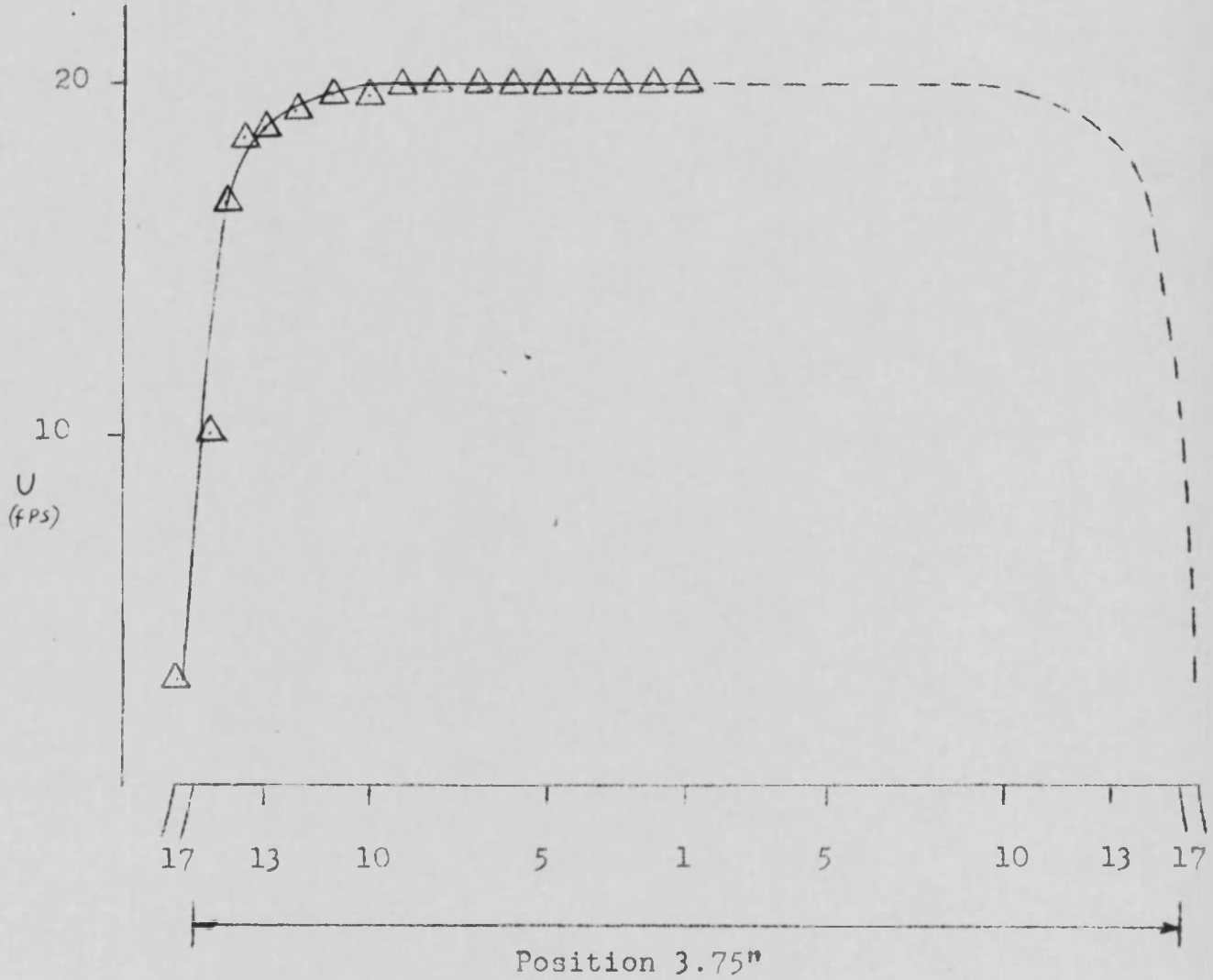

FIGURE 4.3

MEAN VELOCITY PROFILE 1/8" ABOVE NOZZLE

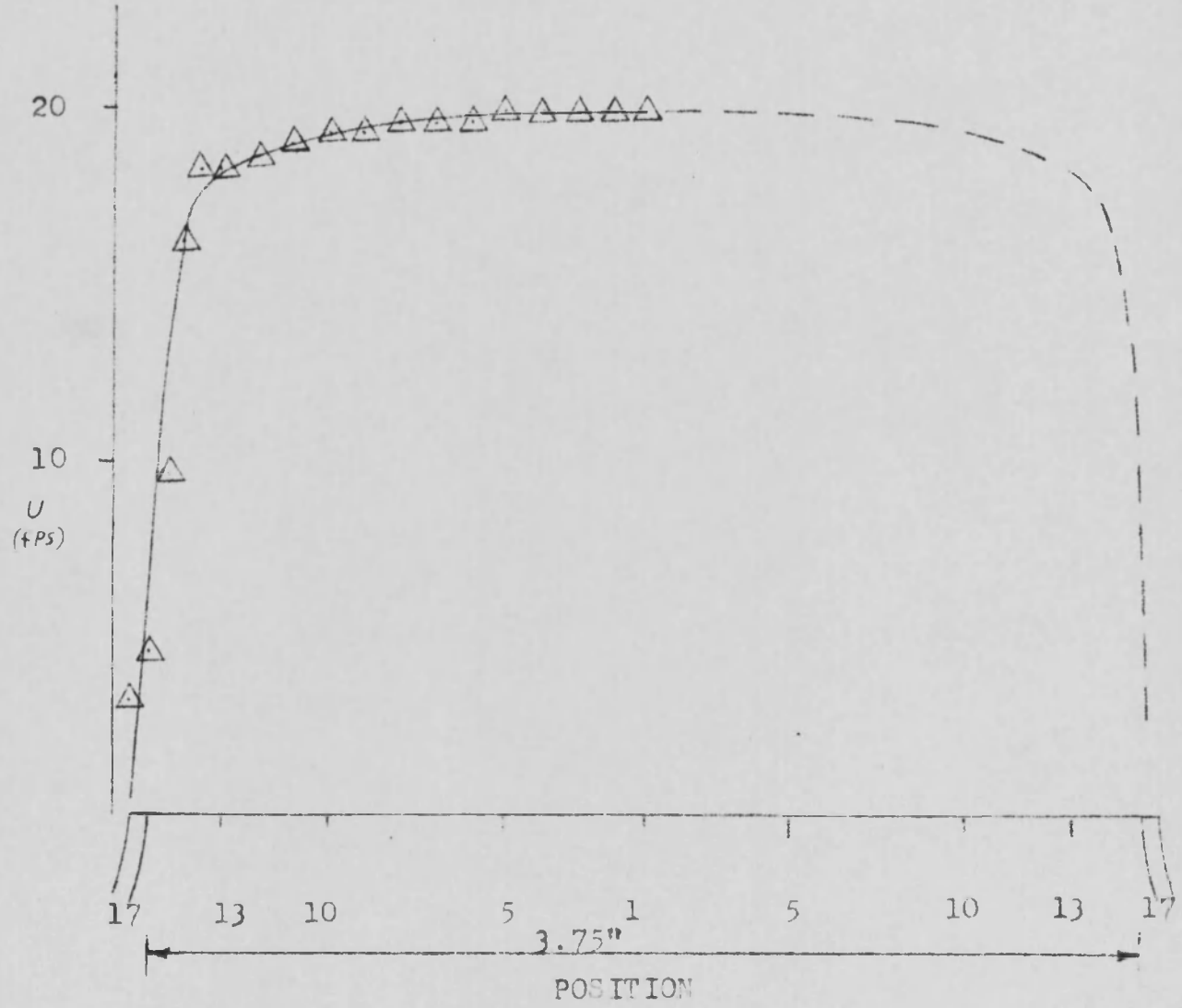

FIGURE 4.4

MEAN VELOCITY PROFILE 1" ABOVE NOZZLE

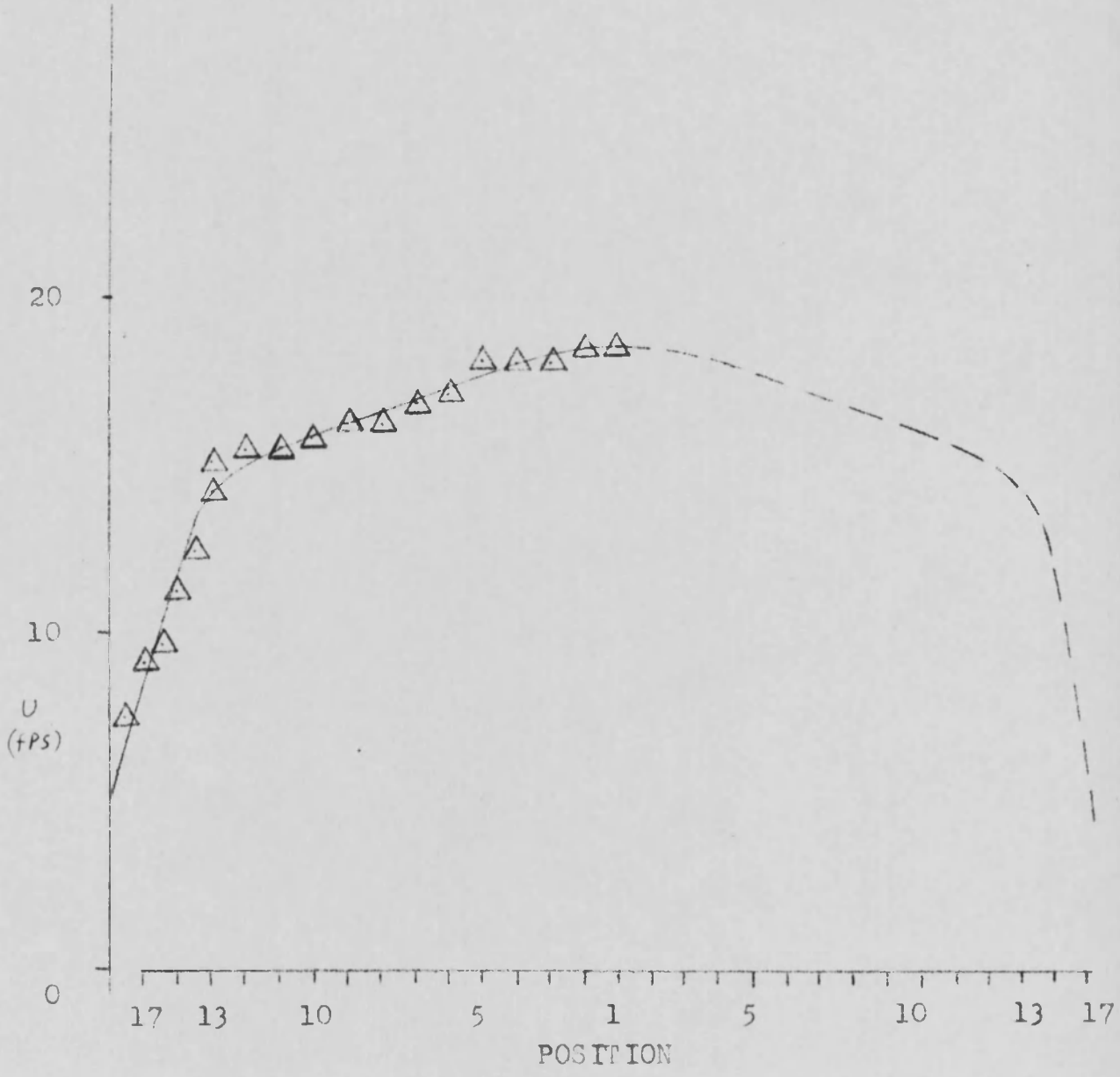

FIGURE 4.5

MEAN VELOCITY PROFILE 2" ABOVE NOZZLE

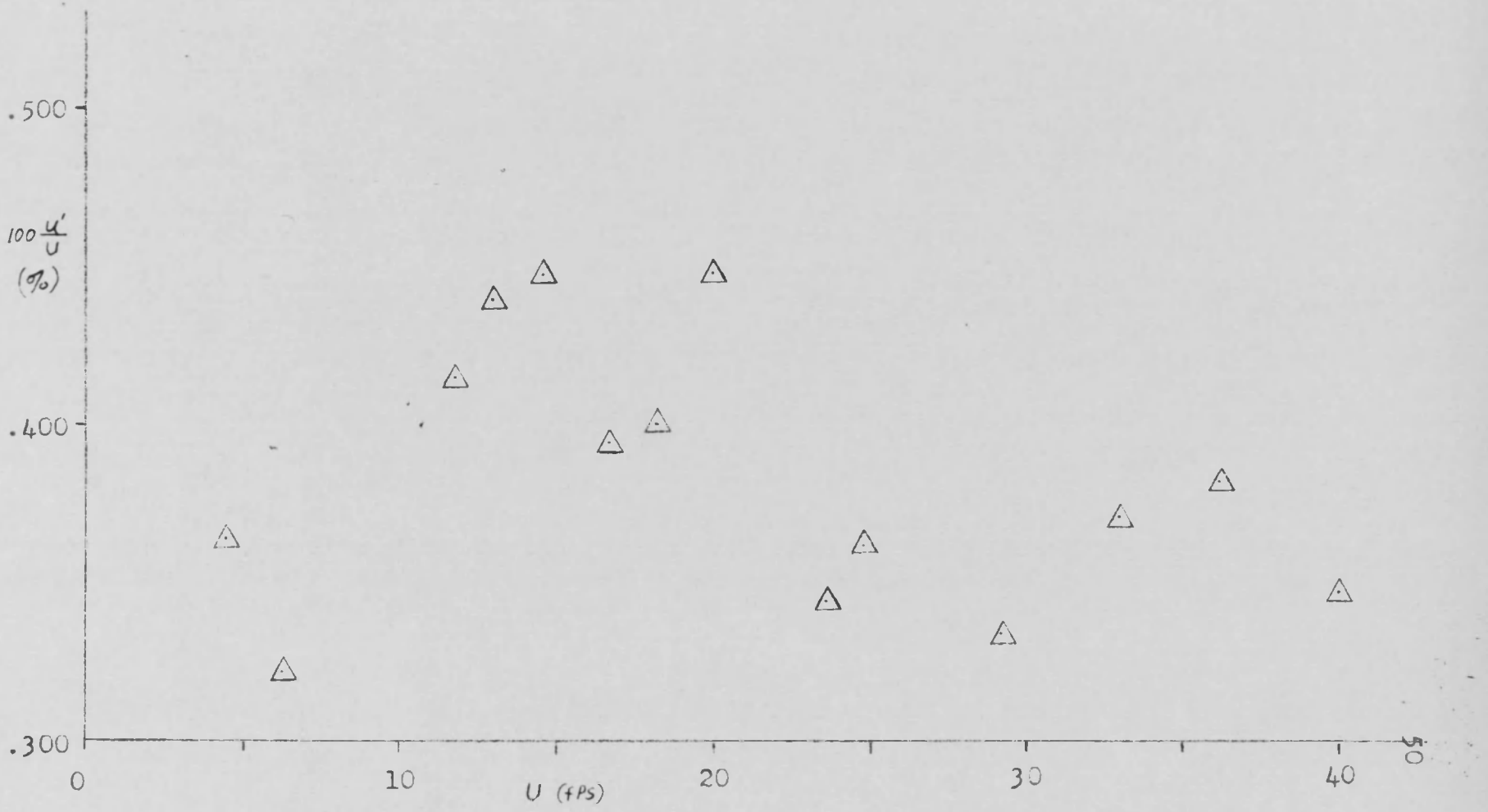

FIGURE 4.6

PERCENT TURBULENCE AT POSITION 1 FROM 0-40 fps

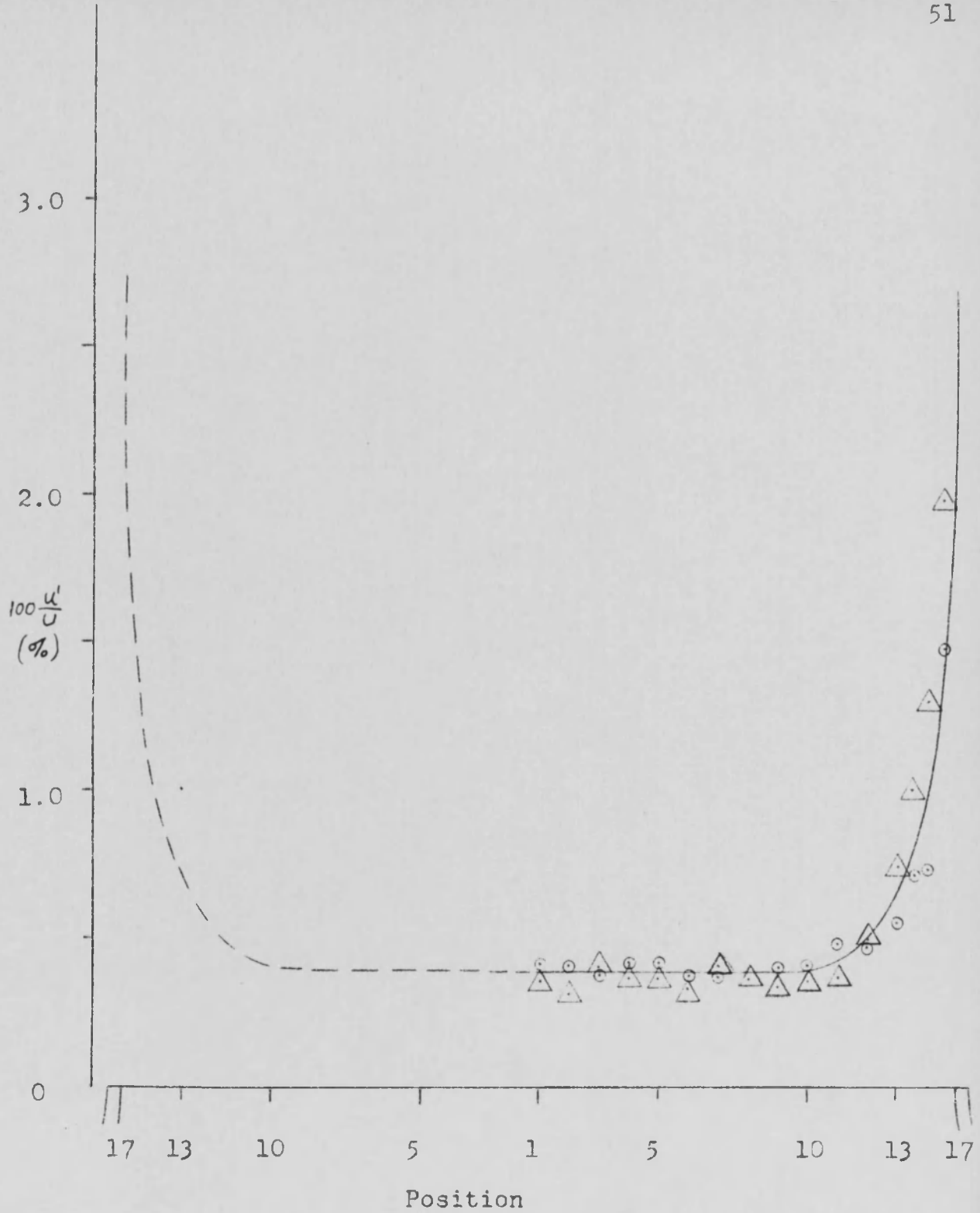

FIGURE 4.7

TURBULENCE PROFILE 1/16" ABOVE NOZZLE

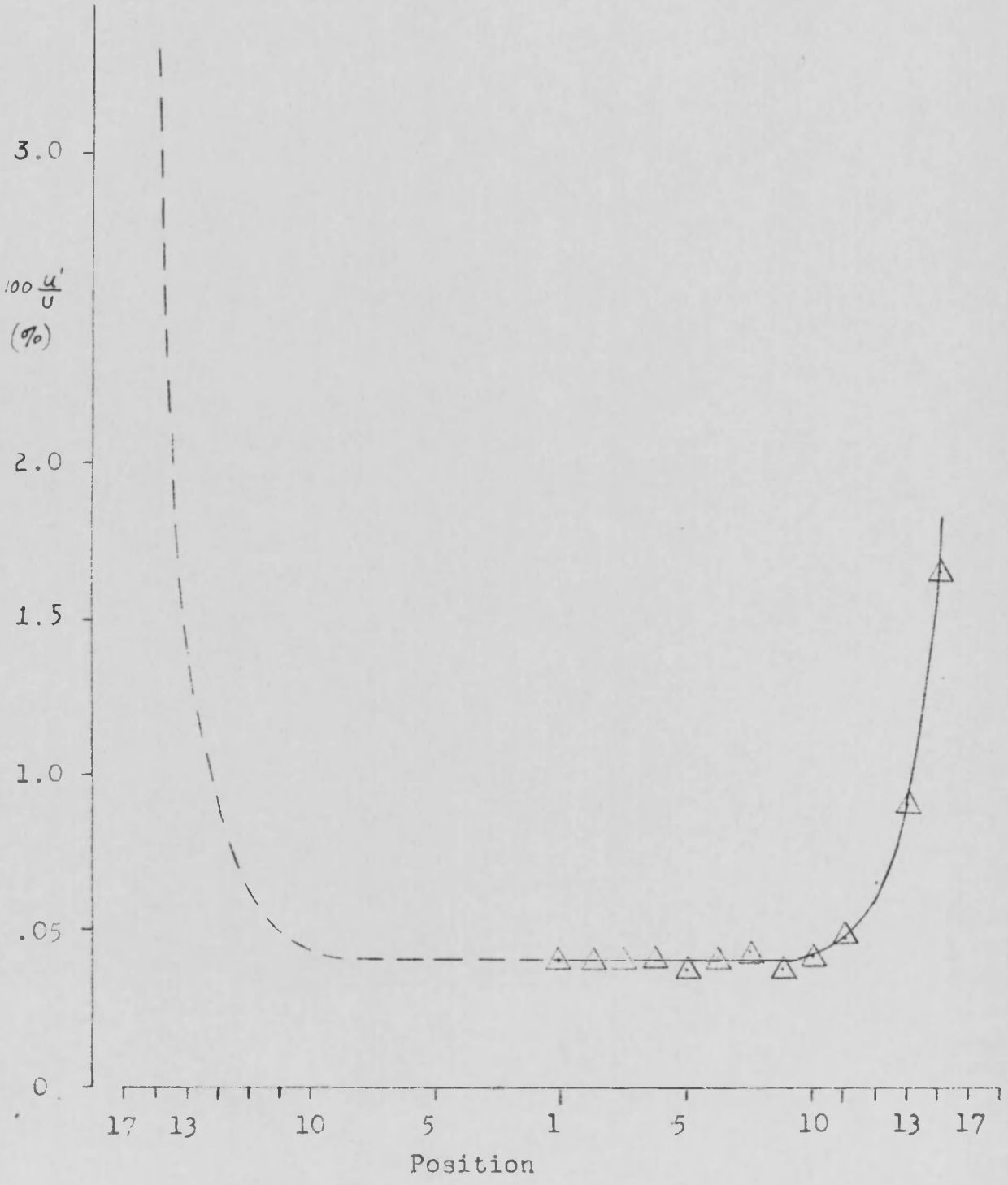

FIGURE 4.8

TURBULENCE PROFILE 1/8" ABOVE NOZZLE

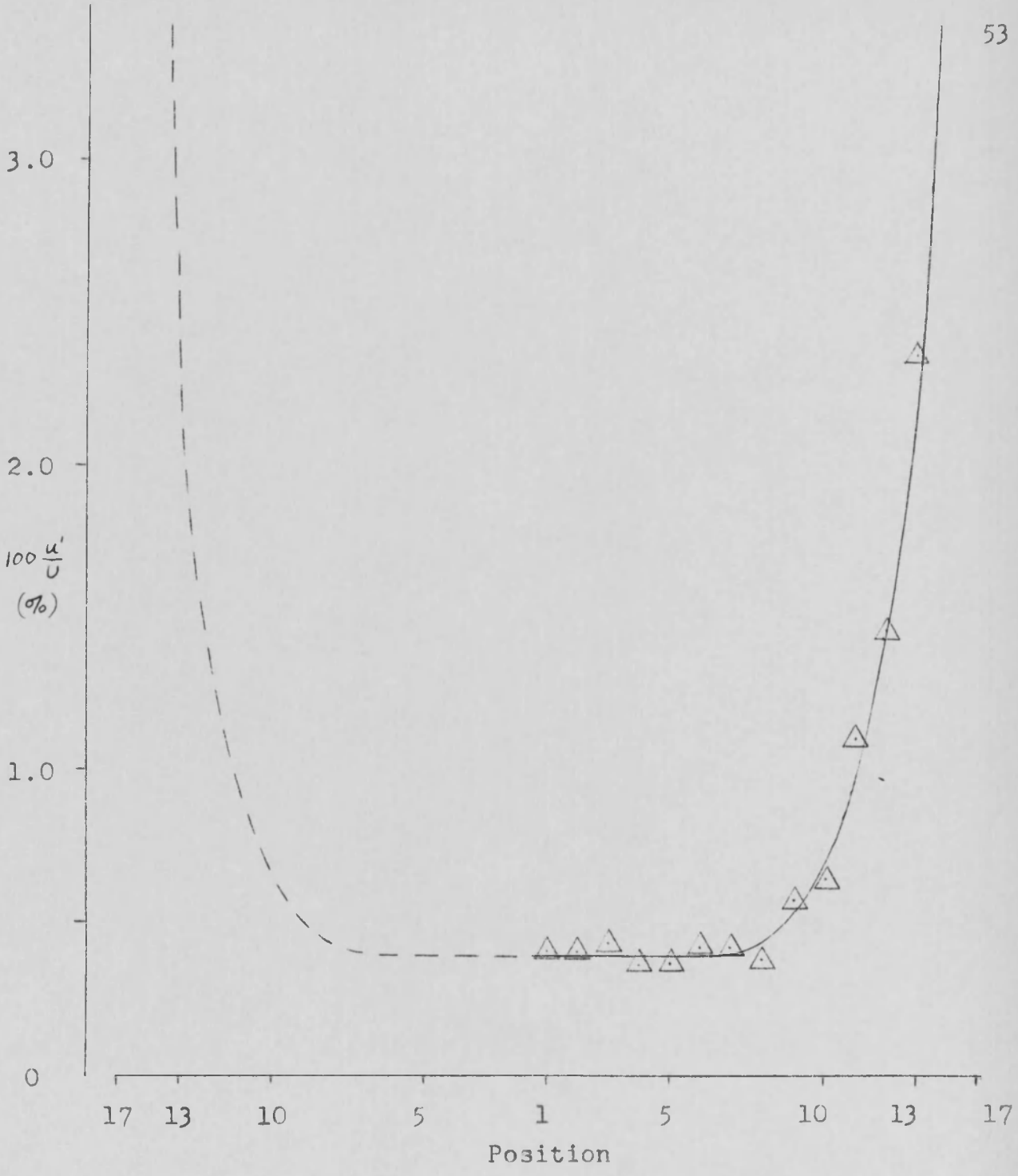

FIGURE 4.9

TURBULENCE PROFILE 1" ABOVE NOZZLE

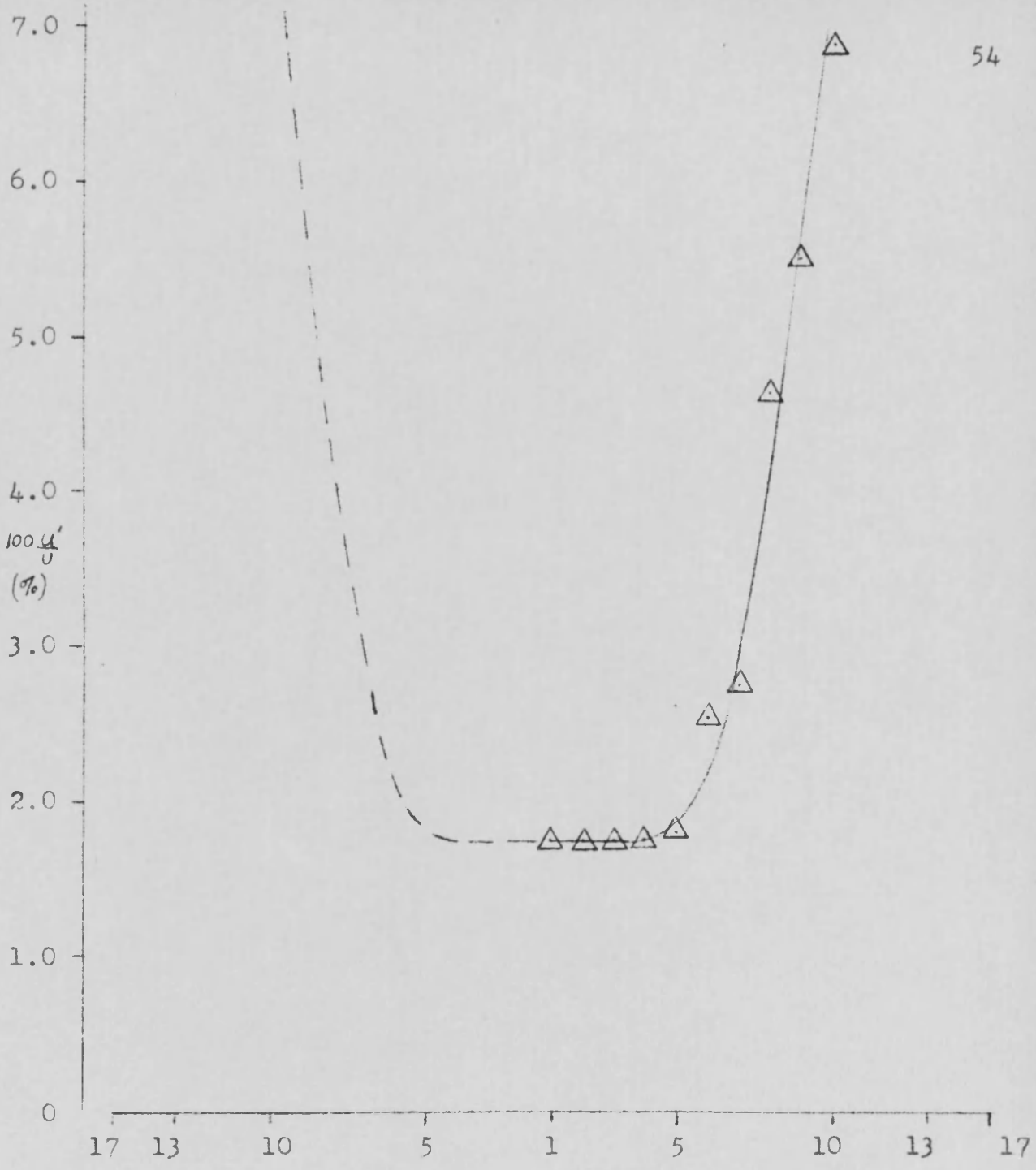

FIGURE 4.10

TURBULENCE PROFILE 2" ABOVE NOZZLE

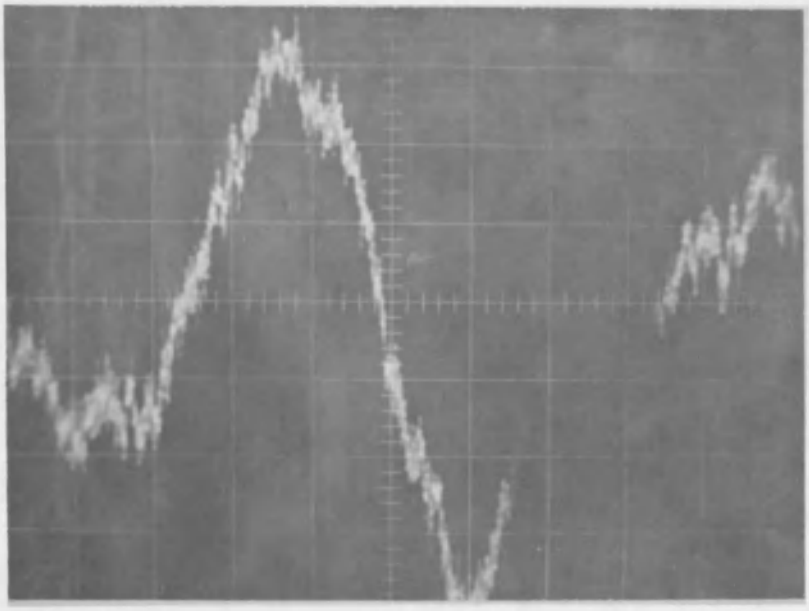

(a) U = 30 fps

(b) U = 20 fps

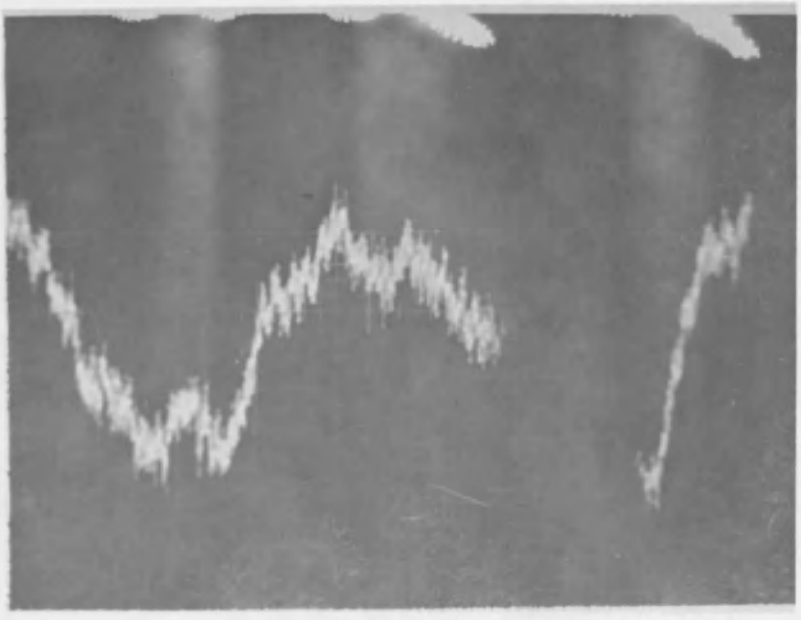

FIGURE 5.1

OSCILLOSCOPE PHOTOGRAPHY OF FLOW DISTURBANCE POSITION 1

TABLE 4.1

HOT WIRE CALIBRATION DATA

Probe 1		Probe 2		Probe 3		Probe 4	
$\bar{I}$	U	$\bar{I}$	U	$\bar{I}$	U	$\bar{I}$	U
1.000	30.00	1.000	30.00	1.000	30.00	1.000	30.00
0.960	28.30	0.950	29.20	0.900	27.70	0.900	26.60
0.920	26.25	0.920	28.00	0.800	25.40	0.800	22.80
0.880	24.40	0.860	26.20	0.700	22.10	0.700	19.50
0.810	22.15	0.820	24.70	0.600	18.70	0.600	16.00
0.760	19.70	0.790	23.85	0.500	16.00	0.500	14.00
0.700	17.25	0.750	22.50	0.400	12.70	0.400	10.80
0.650	15.80	0.710	21.40	0.300	9.60	0.300	8.20
0.600	14.35	0.675	20.40	0.200	6.00	0.200	5.60
0.550	12.25	0.645	19.70	0.100	2.30	0.100	3.50
0.500	10.90	0.605	18.58	0.020	0.00	0.040	0.00
0.450	8.85	0.580	17.70				
0.400	7.88	0.550	16.80				
0.300	4.10	0.510	15.90				
0.200	1.80	0.490	14.90				
0.110	0.00	0.450	13.30				
		0.390	11.70				
		0.310	9.20				
		0.270	8.02				
		0.230	6.65				
		0.190	5.31				
		0.160	3.17				
		0.020	0.00				

TABLE 4.2

CALIBRATION AND TURBULENCE LEVEL DATA

RANGE 0-40 fps 1/16" ABOVE NOZZLE AT

POSITION 1

$\bar{I}$ ma	I ma	U	u' fps	100 u'/U
1.00	1.70	40.00	.1388	.347
.910	1.70	36.25	.1388	.383
.827	1.50	33.00	.1225	.371
.742	1.20	29.25	.098	.335
.630	1.10	24.80	.0898	.362
.572	1.00	23.60	.0816	.346
.484	1.10	20.00	.0898	.448
.440	.90	18.25	.0735	.403
.400	.80	16.75	.0653	.395
.340	.80	14.55	.0653	.448
.310	.70	13.00	.0572	.440
.270	.60	11.80	.0490	.415
.210	.60	8.95	.0490	.548
.140	.25	6.33	.0204	.322
.110	.20	4.47	.0163	.365

PROBE #4

$A = 40.8 \times 10^3$

$B = 0.002$

TABLE 4.3

TURBULENCE DATA 1/16" ABOVE NOZZLE

Position	$\bar{I}$ ma	I ma	U fps	u'fps	100 u'/U
1	.750	1.4	20.00	.0837	.418
2	.750	1.4	20.00	.0837	.418
3	.750	1.3	20.00	.0769	.384
4	.750	1.4	20.00	.0837	.418
5	.750	1.4	20.00	.0837	.418
6	.750	1.3	20.00	.0769	.384
7	.750	1.3	20.00	.0769	.384
8	.750	1.3	20.00	.0769	.384
9	.750	1.4	20.00	.0837	.418
10	.750	1.4	20.00	.0837	.418
11	.740	1.6	20.00	.0946	.473
12	.735	1.6	19.50	.0946	.482
13	.730	1.8	19.00	.1065	.560
14	.720	2.2	18.00	.1300	.723
15	.700	2.1	17.00	.1242	.731
16	.680	4.0	16.00	.2365	1.480
17	.500	8.0	11.00	.4730	4.300
18	.120	2.4	0.00	.1420	100.000

PROBE #2

$A = 29.6 \times 10^3$

B = 0.002

TABLE 4.4

TURBULENCE DATA 1/16" ABOVE NOZZLE

Position	I ma	I ma	U fps	u'fps	100 u'/U
1	.650	1.2	20.00	.0742	.371
2	.650	1.0	20.00	.0618	.305
3	.650	1.3	20.00	.0804	.402
4	.650	1.2	20.00	.0742	.371
5	.650	1.2	20.00	.0742	.371
6	.650	1.1	20.00	.0680	.340
7	.650	1.3	20.00	.0804	.402
8	.650	1.2	20.00	.0742	.371
9	.650	1.1	20.00	.0680	.340
10	.650	1.2	20.00	.0742	.371
11	.640	1.2	19.70	.0742	.376
12	.640	1.6	19.70	.0984	.507
13	.630	2.4	19.40	.1485	.755
14	.590	3.0	18.15	.1855	1.025
15	.550	3.6	16.90	.2225	1.315
16	.460	3.5	11.10	.2165	1.950
17	.250	5.2	7.70	.3215	4.170
18	.100	4.0	3.00	.2470	8.240

PROBE #1

$A = 30.8 \times 10^3$

$B = 0.002$

TABLE 4.5

TURBULENCE DATA 1/8" ABOVE NOZZLE

Position	I ma	I ma	U fps	u'fps	100 u'/U
1	.640	1.3	20.00	.0813	.407
2	.640	1.3	20.00	.0813	.407
3	.640	1.3	20.00	.0813	.407
4	.640	1.3	20.00	.0813	.407
5	.640	1.2	20.00	.0750	.375
6	.640	1.3	20.00	.0813	.407
7	.640	1.4	20.00	.0875	.437
8	.640	1.2	20.00	.0750	.375
9	.640	1.3	20.00	.0813	.407
10	.630	1.5	19.70	.0938	.477
11	.630	2.5	19.70	.1562	.794
12	.621	2.8	19.30	.1750	.906
13	.600	5.0	18.80	.3125	1.665
14	.590	13.5	18.50	.844	4.57
15	.530	21.5	16.70	1.345	8.05
16	.300	33.6	10.00	2.100	21.00
17	.200	20.0	6.50	1.25	19.25
18	.100	12.5	3.10	.7810	25.2

PROBE #3

A = 31.25

B = 0.002

TABLE 4.6

TURBULENCE DATA 1" ABOVE NOZZLE

Position	I ma	I ma	U fps	u' fps	100 u'/U
1	.640	1.3	20.00	.0813	.407
2	.640	1.3	20.00	.0813	.407
3	.640	1.4	20.00	.0875	.438
4	.640	1.2	20.00	.0750	.375
5	.640	1.2	20.00	.0750	.375
6	.630	1.3	19.70	.0813	.413
7	.630	1.3	19.70	.0813	.413
8	.630	1.2	19.70	.0750	.380
9	.621	1.8	19.40	.1125	.580
10	.620	2.0	19.40	.1250	.644
11	.610	3.4	19.05	.2125	1.115
12	.600	4.4	18.75	.2750	1.468
13	.590	7.0	18.45	.4375	2.370
14	.590	14.8	18.45	.9250	5.010
15	.520	22.0	16.25	1.375	8.460
16	.310	32.0	9.69	2.000	20.65
17	.150	20.0	4.69	1.250	26.70
18	.100	11.6	3.15	.7250	23.00

PROBE #3

A = 31.25

B = 0.002

TABLE 4.7

TURBULENCE DATA 2" ABOVE NOZZLE

Position	I ma	I ma	U fps	u'fps	100 u'/U
1	.590	5.2	18.45	.326	1.77
2	.590	5.2	18.45	.326	1.77
3	.580	5.1	18.15	.319	1.76
4	.580	5.1	18.15	.319	1.76
5	.580	5.2	18.15	.326	1.80
6	.550	7.0	17.2	.438	2.55
7	.540	7.5	16.9	.469	2.77
8	.520	12.0	16.26	.752	4.62
9	.520	14.4	16.26	.902	5.55
10	.510	17.6	15.95	1.100	6.89
11	.500	20.8	15.64	1.300	8.30
12	.500	25.6	15.64	1.600	10.25
13	.480	32.8	15.1	2.050	13.58
14	.400	33.6	12.5	2.100	16.80
15	.360	38.4	11.26	2.400	21.30
16	.310	36.8	9.7	2.300	23.70
17	.290	36.8	9.07	2.300	25.40
18	.240	32.0	7.5	2.000	26.70

PROBE #4

A = 31.3

B = 0.002

BIBLIOGRAPHY

1. Lewis, and von Elbe, Combustion and Flame Explosions of Gases, Academic Press Co., New York, N. Y., 1951.

2. Dryden, H. L., Measurements of Intensity and Scale of Wind Tunnel Turb and Their Relation to Critical Mach Number of Spheres. NACA, No. 581, 1937.

3. Batchelor, G. K., Theory of Homogeneous Turbulence, Cambridge University Press, Cambridge, Mass., 1959.

4. Harrop, R., A Method for Designing Wind Tunnel Contractions, Journal of Roy. Aero. Soc., London, March, 1951.

5. Hicks, N., M. S. Thesis, The University of Arizona.

6. Dean, R. C., Jr., Aerodynamic Measurements, Eagle Enterprises, Boston, Mass., 1954.

7. Knudsen, and Katz, Fluid Dynamics and Heat Transfer, McGraw-Hill Co., New York, N. Y., 1958.

8. Jacob, M., and Hawkins, G. A., Elements of Heat Transfer, Wiley & Sons, New York, N. Y., 1959.

9. McAdams, W. H., Heat Transmission, McGraw-Hill Co., New York, N. Y., 1954.

10. Lion, K. S., Instrumentation in Scientific Research, McGraw-Hill Co., New York, N. Y., 1959.

11. Flow Corporation, Bulletin Number 9, Boston, Mass., 1958.

12. Flow Corporation, Bulletin Number 11, Boston, Mass., 1959.

13. Hubbard, P. G., Operating Manual for the IIHR Hot Wire and Hot Film Anemometer, University of Iowa Press, 1957.

BIBLIOGRAPHY

Additional References

1. Lowell, H. H., Design and Application of Hot Wire Anemometers for Steady-State Measurements at Transonic and Supersonic Airspeeds, NACA No. 932, Washington, 1950.

2. Rockett, J. A., Design of a Combustion Tunnel, Harvard University, Cambridge, Mass., March 1955.